Mathematical Biology

Geometry and topology of parameter space: investigating measures of robustness in regulatory networks

**Madalena Chaves · Anirvan Sengupta ·
Eduardo D. Sontag**

Abstract The concept of robustness of regulatory networks has been closely related to the nature of the interactions among genes, and the capability of pattern maintenance or reproducibility. Defining this robustness property is a challenging task, but mathematical models have often associated it to the volume of the space of admissible parameters. Not only the volume of the space but also its topology and geometry contain information on essential aspects of the network, including feasible pathways, switching between two parallel pathways or distinct/disconnected active regions of parameters. A method is presented here to characterize the space of admissible parameters, by writing it as a semi-algebraic set, and then theoretically analyzing its topology and geometry, as well as volume. This method provides a more objective and complete measure of the robustness of a developmental module. As a detailed case study, the segment polarity gene network is analyzed.

Mathematics Subject Classification (2000) 92-08 · 93B27 · 93B35

M. Chaves
Projet COMORE, INRIA Sophia Antipolis, 2004 Route des Lucioles,
BP 93, 06902 Sophia Antipolis, France
e-mail: mchaves@sophia.inria.fr

A. Sengupta
BioMaPS Institute for Quantitative Biology and Department of Physics,
Rutgers University, Piscataway, NJ 08854, USA
e-mail: anirvans@physics.rutgers.edu

E. D. Sontag (✉)
BioMaPS Institute for Quantitative Biology and Department of Mathematics,
Rutgers University, Piscataway, NJ 08854, USA
e-mail: sontag@math.rutgers.edu

1 Introduction

For biological networks, the concept of robustness often expresses the idea that the system's regulatory functions should operate correctly under a variety of situations. The network should respond appropriately to various stimulii and recognize meaningful ones (either harmful or favorable), but it should also ignore small (not meaningful) variations in the environment as well as inescapable fluctuations in the abundances of biomolecules involved in the network [1–3].

While it is difficult to define this robustness property in a precise form, it has been associated to the space of admissible kinetic parameters, its volume [3], and the effect of paramater perturbations on the qualitative behavior of the system [1,2,4]. Some methods for parameter sensitivity have been developed [5,6], based essentially on derivatives of variables or fluxes with respect to the system's parameters. The volume of the parameter space can be used as an indication of "how many" parameter combinations are possible, and these are related to the ability of the network to work under a variety of situations. For instance, parameters may range through different orders of magnitude, representing very different environments. A small parameter space volume is a clear indication of low robustness, as the model will require precise tuning to reproduce any features. Hence robustness is associated to larger volumes. However, size may not always be a reliable measure for robustness; other quantities, such as shape, also play a very significant role, as illustrated in Fig. 1. In the context of systems with uncertain parameters, for instance, it is quite useful to have an idea of the distribution, or shape, of the sets of good or bad parameters. In [4] statistical analysis of a chemotaxis network indicates that there are two regions of the uncertain parameter space with a high concentration of bad parameters (thus suggesting a feasible parameter
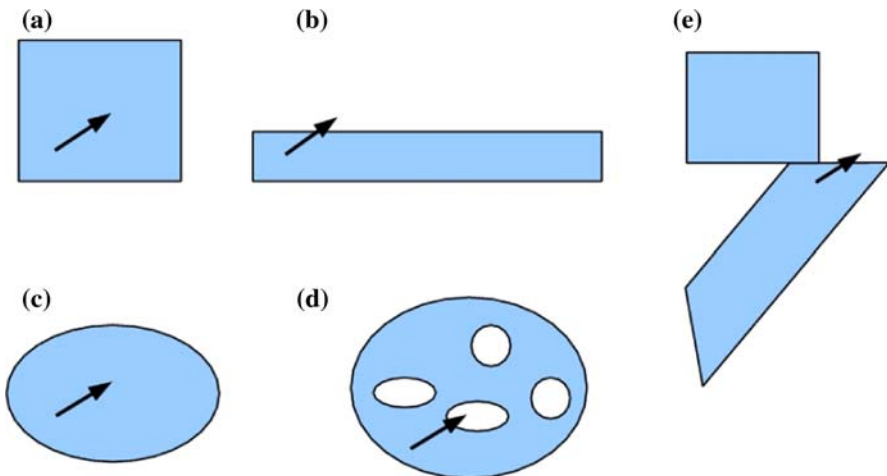
Fig. 1 The role of geometry and topology in robustness. Regions **a** and **b** have the same volume, but **b** is less robust: the same perturbation leads out of the space. Regions **c** and **d** also have the same volume, but **d** is not a simply connected set, hence less robust. Region **e**, although connected, is composed of two pieces that touch only along a small face

space of the form Fig. 1d). Analysis of the shape or geometry of the admissible parameter set gives an indication not only of its size, but also how far perturbations around each parameter disrupt the network. A robust biological network will admit small fluctuations in its parameters without changing its qualitative behavior. So, a robust network will be associated to a system whose parameter set has few "narrow pieces" and "sharp corners". In such sets, reasonable parameter fluctuations may occur without leaving the set, hence maintaining the network's qualitative behavior (compare Fig. 1a, b). The topology, and in particular the simple-connectedness or not of the feasible parameter set is also important (compare Fig. 1c, d). However, even if the set is connected, it may exhibit low robustness if it is composed of several pieces with lower dimension connecting faces, as in Fig. 1e. In fact, as will be seen later, this is one of the situations that happen in our example.

To illustrate the importance of parameter space geometry, and the insight it brings to understanding the network, the model of the segment polarity network developed by von Dassow and collaborators [3] will be analyzed as a "case study" of our approach. The segment polarity network is part of a cascade of gene families responsible for generating the segmentation of the fruit fly embryo [7]. Genes in earlier stages are transiently expressed, but the segment polarity genes maintain a stable pattern for about three hours. It has been suggested that the segment polarity genes constitute a robust developmental module, capable of autonomously reproducing the same behavior or generating the same gene expression pattern, in response to transient inputs [3,8,9]. This robustness would be due to the nature of interactions among genes, rather than the kinetic parameters of the reactions. The model [3] describes the interactions among the principal segment polarity genes, is continuous, and involves cell-to-cell communications and around 50 parameters which are essentially unknown. The authors of [3] explored the model by randomly choosing 240,000 parameter sets out of which about 1,192 (or 0.5%) sets were consistent with the generation (at steady state) of the wild type pattern. To explore the robustness of the network as a property of its interactions, Albert and Othmer [9,10] developed a Boolean model of the segment polarity network, a discrete logical model where each species has only two states (0 or 1; "OFF" or "ON"), but no kinetic parameters need to be defined. This Boolean model is amenable to various methods for systematic robustness analysis [11–13]. Ingolia [8] focused on the properties of the (slightly changed) model [3] in individual cells, such as bistability, and extrapolated necessary conditions on parameters to the full intercellular model.

We propose a different approach, that *retains the information contained on the kinetic parameters*, but partially approximates the model by a logical form with various possible ON levels and species-dependent activation parameters. The admissible set of parameters of the model [3] is analyzed by constructing a cylindrical algebraic decomposition. Among other conclusions, our analysis completely explains the two "missing links" in von Dassow et al. original model, namely: why the segment polarity pattern can not be recovered without the negative regulation of *engrailed* by Cubitus repressor protein, and why the autocatalytic *wingless* activation pathway vastly increases the network robustness.

The present approach shows that, in contrast to volume only estimates, the topology and geometry of parameter sets provide reliable quantitative measures of robustness of

a system. Some of our work may be seen as a "global" counterpart to the local analysis done in [14] in which eigenvector analysis was used to study the "stiff/sloppy" character of good parameter sets. In separate work [15], we study evolutionary implications of the geometric structure, with a focus on a measure of robustness that is related to having low rate of exit from the region under random walk [16].

2 The segment polarity network model

The principal segment polarity genes [7] are *engrailed* (*en*), *wingless*, *patched*, *cubitus interruptus* and *hedgehog*. The wild type expression pattern for these five segment polarity genes is experimentally well characterized, and is stably maintained for a period of about three hours (approximately during stages 8–11 of embryonic development) [17]. The pattern is periodically repeated (every four cells, in the early stages 6–8 of embryonic development), and defines the positions of the parasegments in the embryo of the fly. In wild type, both *engrailed* and *hedgehog* are expressed in every third cell [18], while *wingless* is expressed in every cell anterior to an *en*-expressing cell [18]. Further experimental observations show that *cubitus* is expressed in all but the cell expressing *en* [19], and *patched* is strongly expressed in every cell surrounding *en*-expressing cells [18], but not expressed in *en*-expressing cells. The boundaries of the parasegments are formed between the two cells expressing *wingless* and *engrailed*.

The model proposed by von Dassow et al. [3] (Appendix B) describes the concentrations of these five mRNAs and corresponding proteins in a four cell parasegment of the fly embryo, subject to periodic boundary conditions (see also Fig. 6). From now on, each cell is assumed to have a square shape, with four faces (see Appendix E). Nine of these mRNAs and proteins are considered to have a homogeneous concentration throughout each cell: engrailed mRNA and protein (*en* and EN), wingless mRNA and (internal) protein (*wg* and IWG), patched mRNA (*ptc*), cubitus mRNA, active and repressor proteins (*ci*, CI, and CN), and hedgehog mRNA (*hh*). Each of these variables has a distinct concentration in each cell (X_i, $i = 1, \ldots, 4$). In addition, there are three other proteins whose concentration varies in each of the four cell faces: external wingless protein (EWG), patched protein (PTC) and hedgehog protein (HH). For each of these variables, the concentration in cell i at face j is denoted $X_{i,j}$, $i = 1, \ldots, 4$, $j = 1, \ldots, 4$. Thus, overall there are: $n = 9 \times 4 + 3 \times 4 \times 4 = 84$ variables. Throughout the paper, the following notation will be used (prime denotes transpose):

$$X = (X_1, X_2, X_3, X_4)', \quad \text{for} \quad X \in \{en, \text{EN}, wg, \text{IWG}, ptc, ci, \text{CI}, \text{CN}, hh\}.$$

and

$$X = (X_{1,1}, X_{1,2}, X_{1,3}, X_{1,4}, X_{2,1}, \ldots, X_{4,4})', \quad \text{for} \quad X \in \{\text{EWG}, \text{PTC}, \text{HH}\}.$$

The full vector of concentrations is:

$$x = (en', \text{EN}', wg', \text{IWG}', \text{EWG}', ptc', \text{PTC}', ci', \text{CI}', \text{CN}', hh', \text{HH}').$$

To formulate the mathematical model, define a vector of species concentrations ($x \in \mathbb{R}^n_{\geq 0}$) and a parameter vector ($p \in \mathbb{R}^r_{\geq 0}$), together with a set of outputs ($y \in \mathbb{R}^m_{\geq 0}$, the measured gene expression levels). Introduce functions $f : \mathbb{R}^n_{\geq 0} \times \mathbb{R}^r_{\geq 0} \to \mathbb{R}^n$ and $h : \mathbb{R}^n_{\geq 0} \to \mathbb{R}^m_{\geq 0}$, where $\mathbb{R}_{\geq 0} = \{x \in \mathbb{R} : x_i \geq 0, \text{ for all } i\}$, and consider the system with outputs

$$\frac{dx}{dt} = f(x, p) \tag{1}$$

$$y = h(x) \tag{2}$$

where the function $h(x)$ could be, for instance, a vector listing the concentration of *wingless*, *engrailed*, and other of the segment polarity mRNAs which have been experimentally measured. Or, in other words, y is "the phenotype corresponding to the genotype x". The function f is, for instance, as shown in Appendix B for von Dassow et al.'s model. The wild type expression pattern for the segment polarity genes can be viewed as (one of) the steady state solution of system (1).

2.1 The wild type pattern set

An output function is typically composed of variables (or combinations of variables) that are *known or available from measurements*. Following [3,9] (and references therein), as well as the discussion above, the wild type expression pattern, in each group of four cells, is characterized mainly by the expression of *engrailed*, *hedgehog*, and *wingless*. Here we will further add expression of *cubitus* and *patched* to incorporate further experimental evidence [18,19]. These five mRNAs are among the most well documented, so we will consider the output function $h : \mathbb{R}^n_{\geq 0} \to \mathbb{R}^{20}_{\geq 0}$ to be the state of these five variables. In addition, experimental data is typically of the form "expressed"/"not expressed", which may be best translated as "0" if concentration is below a certain threshold ε, or "1" if concentration is above the threshold. Then we have:

$$y = h(x) = \begin{pmatrix} h_{en}(x) \\ h_{hh}(x) \\ h_{wg}(x) \\ h_{ci}(x) \\ h_{ptc}(x) \end{pmatrix} = \begin{pmatrix} \text{sign}_\varepsilon(en) \\ \text{sign}_\varepsilon(hh) \\ \text{sign}_\varepsilon(wg) \\ \text{sign}_\varepsilon(ci) \\ \text{sign}_\varepsilon(ptc) \end{pmatrix}, \tag{3}$$

where $\text{sign}_\varepsilon(r) = 0$ if $r < \varepsilon$ and $\text{sign}_\varepsilon(r) = 1$ if $r \geq \varepsilon$. From experimental measurements, the wild type phenotype is characterized as follows. It is well known [17] that both *en* and *hh* are expressed in every third cell, so the desired steady state outputs for these variables are

$$h_{en}(x) = (0, 0, 1, 0)', \quad h_{hh}(x) = (0, 0, 1, 0)', \quad \text{for } x \in \mathbb{R}^n. \tag{4}$$

Wingless mRNA is only expressed in every second cell, to the left of *en*, so that its desired steady state output is

$$h_{wg}(x) = (0, 1, 0, 0)', \quad \text{for } x \in \mathbb{R}^n. \tag{5}$$

Cubitus and patched mRNAs are typically expressed in all but those cells expressing *en* [18,19], so the desired steady state output for *ci* and *ptc* is of the form:

$$h_{ci}(x) = (1, 1, 0, 1)', \quad h_{ptc}(x) = (1, 1, 0, 1)', \quad \text{for } x \in \mathbb{R}^n. \tag{6}$$

The boundaries of the parasegments are expected to form between every second and third cells. The set that contains all states which yield an output satisfying (4)–(6) will be the set representing the wild type pattern for the segment polarity model (Appendix B). From the definition of h (and taking into account the assumptions below for simplicity of analysis), the set of wild type states is of the form:

$$\begin{aligned}
\mathcal{W} = \{x \in \mathbb{R}^n_{\geq 0} : \ & en = (0, 0, N_3, 0)', \ hh = (H_1, H_2, H_3, H_4)', \\
& wg = (W_1, W_2, W_3, W_4)', \\
& ci = (U_1, U_2, 0, U_4)', \ ptc = (T_1, T_2, T_3, T_4)', \\
& \text{with } W_4 < W_{1,3}; \ W_{1,3,4}, H_{1,2,4} < \varepsilon; \ W_2, N_3, H_3 \geq \varepsilon; \\
& T_4 = T_2; \ T_{1,2}, U_{1,2,4} \geq \varepsilon; \ T_3 < \varepsilon; \}.
\end{aligned} \tag{7}$$

The value ε is a threshold for mRNA (or protein) concentration above which the gene (or protein) is considered expressed. In [3] it was assumed that a gene/protein is expressed when it reaches 10% of its maximal concentration. As discussed below, in the model discussed in this paper the maximal concentration will be 1, hence we will set $\varepsilon = 0.1$.

Remark For simplicity, we have imposed some additional conditions when writing down the set $\mathcal{W}$, compared to merely asking that (4)–(6) hold. These conditions are:

$$\begin{aligned}
& en_i = 0, \quad i = 1, 2, 4 \ \text{ rather than } \ en_i < \varepsilon \\
& ci_3 = 0 \ \text{ rather than } \ ci_3 < \varepsilon \\
& wg_4 \leq \min\{wg_1, wg_3\} \\
& ptc_4 = ptc_2.
\end{aligned}$$

These are mild assumptions which however allow many analytic calculations to be carried out explicitly (further discussion can be found in Appendix H), and provide intuition into the dynamics of the segment polarity model. Furthermore, as will become clear in our analysis, these assumptions are verified for many sets of feasible parameters—more precisely, for all sets of parameters except in subsets of lower dimension.

3 Steady states define the feasible parameter space

Previous studies [3,8] have tested the parameter space by randomly choosing sets of parameters and simulating the continuous model. If the corresponding trajectory reaches a steady state, and if this steady state is compatible with the experimentally observed wild type gene pattern, then the given set of parameters is said to be a "solution" to the modeling problem.

A more efficient and complete study of the parameter space can be devised, by first solving the algebraic equations of the model at steady state, and writing the steady state solutions as a function of the parameters. On the other hand, the steady state solutions are known—the set of elements representing the wild type pattern is denoted by $\mathcal{W}$—so, one can then look for parameters that yield this pattern. Since many sets of parameters may be expected to yield the wild type pattern, this procedure provides a family of conditions defining regions of "good"or feasible parameters "p" for wild type steady states $x \in \mathcal{W}$.

The problem of characterizing the sets of feasible parameters is then reduced to finding all possible parameter vectors p which correspond to a system having a steady state in $\mathcal{W}$.

This will be the set of "good" parameters:

$$G = \{p \in \mathbb{R}^r_{\geq 0} : \exists x \in \mathcal{W} \text{ s.t. } f(x, p) = 0\}. \tag{8}$$

3.1 Large Hill coefficients: approximating the continuous model

To find the set G, a straightforward approach would be to solve the steady-state equations for the original system, thus obtaining expressions for x in terms of p:

$$f(x, p) = 0 \iff x = F(p),$$

and compare these expressions to the desired form (in $\mathcal{W}$):

$$F(p) \in \mathcal{W} \iff p \in G.$$

A possible drawback of this method is that explicit solutions $x = F(p)$ for the original system and then explicit formulas for G may not be easy to compute. On the other hand, many of the equations in the model [3] involve terms of the form (see also Appendix B):

$$\phi(X, \kappa, \nu) = \frac{X^\nu}{\kappa^\nu + X^\nu} \quad \text{or} \quad \psi(X, \kappa, \nu) = \frac{\kappa^\nu}{\kappa^\nu + X^\nu},$$

meaning that, if species X is above a certain threshold κ, the function ϕ is active (ON), but the function ψ is inactive (OFF). The exponent ν, also known as the Hill coefficient, characterizes the steepness of an OFF/ON transition.

As found in [20], the model is more robust when the coefficients ν are large. Indeed, for ν in the interval [5.0, 10.0], together with some constraints on other parameters

(as detailed in Table 1 in [20]), the proportion of "good parameters" sets increased to 4 out of 5. For large enough exponents, this saturation function becomes very steep, and ϕ becomes practically insensitive to the actual value of ν. Let ν be very large and approximate ϕ by a step function: it is not unreasonable to expect this approximation to capture a large part of the feasible parameter space. This is also the basis of the typical on/off logical interpretation of gene expression. Any such term $\phi(X, \kappa, \nu)$, for large ν, may thus be replaced by a multivalued step function of the form:

$$\theta^+(X, \kappa) = \begin{cases} 0, & X < \kappa \\ [0, 1], & X = \kappa \\ 1, & X > \kappa . \end{cases} \tag{9}$$

Define also the symmetric step function $\theta^-(X, \kappa) = 1 - \theta^+(X, \kappa)$. The approximation of $\phi(X, \kappa, \nu)$ by a step function inevitably has a discontinuity at $X = \kappa$. Defining θ^+ to be multivalued at κ is one way to represent all the states that the function ϕ may take as X is in smaller and smaller neighborhoods of κ, as ν becomes larger and larger. Thus:

$$\lim_{\nu \to \infty} \phi(X, \kappa, \nu) = \theta^+(X, \kappa), \quad \lim_{\nu \to \infty} \psi(X, \kappa, \nu) = 1 - \theta^+(X, \kappa) = \theta^-(X, \kappa), \tag{10}$$

where, for $X = \kappa$, we interpret (10) as saying that the corresponding limit belongs to the interval [0, 1]. A composite function of ϕ and ψ also frequently appears in the continuous equations (Appendix B):

$$\phi(X_a \psi(X_b, \kappa_b, \nu_b), \kappa_a, \nu_a).$$

This function can be simplified in terms of step functions to:

$$\theta^+(X_a \theta^-(X_b, \kappa_b), \kappa_a) = \begin{cases} \theta^+(X_a, \kappa_a)\theta^-(X_b, \kappa_b), & X_b \neq \kappa_b \\ \theta^+(X_a[0, 1], \kappa_a), & X_b = \kappa_b, \end{cases} \tag{11}$$

since

$$X_b > \kappa_b \Rightarrow \theta^-(X_b, \kappa_b) = 0 \Rightarrow \theta^+(X_a \theta^-(X_b, \kappa_b), \kappa_a) = \theta^+(0, \kappa_a) = 0,$$
$$X_b = \kappa_b \Rightarrow \theta^-(X_b, \kappa_b) = [0, 1] \Rightarrow \theta^+(X_a \theta^-(X_b, \kappa_b), \kappa_a) = \theta^+(X_a[0, 1], \kappa_a),$$
$$X_b < \kappa_b \Rightarrow \theta^-(X_b, \kappa_b) = 1 \Rightarrow \theta^+(X_a \theta^-(X_b, \kappa_b), \kappa_a) = \theta^+(X_a, \kappa_a).$$

As an example, consider the equation governing *engrailed* from the original model which can be found in [3,20] (or in Appendix B). In this model the concentration of *engrailed* in cell i (en_i), is positively regulated by external Wingless protein (EWG_i) and negatively regulated by Cubitus repressor protein (CN_i) concentrations (further notation is found in Appendix A):

$$\frac{den_i}{dt} = \frac{1}{H_{en}} \left(\phi(\text{EWG}_i \psi(\text{CN}_i, \kappa_{\text{CN}en}, \nu_{\text{CN}en}), \kappa_{\text{WG}en}, \nu_{\text{WG}en}) - en_i \right).$$

For large exponents ν, this simplifies to the equation:

$$\frac{den_i}{dt} = \frac{1}{H_{en}}\left(\theta^+(\text{EWG}_{\underline{i}}\theta^-(\text{CN}_i, \kappa_{\text{CN}en}), \kappa_{\text{WG}en}) - en_i\right).$$

To analyticaly study the space of feasible parameters for the segment polarity network model [3], we will thus consider that all exponents ν are large, and apply method (10) to simplify the original system of equations. In addition, as discussed, the system is assumed to be at steady state, in which case the gene expression pattern must satisfy:

$$en_i = \theta^+(\text{EWG}_{\underline{i}}\theta^-(\text{CN}_i, \kappa_{\text{CN}en}), \kappa_{\text{WG}en}).$$

Applying (10) and then solving the system at steady state yields the set of algebraic equations (52)–(63), which characterize the gene expression pattern of the segment polarity network according to our approximation of the von Dassow et al. model. In particular, note that the cubitus mRNA equation becomes

$$ci_i = U_i\theta^-(\text{EN}_i, \kappa_{\text{EN}ci}), \quad i = 1, \ldots, 4,$$

where the choice of the parameters $U_i \in [0, 1]$ is explained in Appendix C. Furthermore, in characterizing the set of feasible parameters, it will become clear that allowing distinct U_i enlarges the space of possible parameters. Asymmetry in *cubitus* expression (i.e., distinct values U_i for each $i = 1, \ldots, 4$) could be due, for instance, to some of the pair rule genes. Sloppy paired, or a combination of Runt and Factor X, regulate the transition from pair rule to segment polarity genes expression, and induce asymmetric anterior/posterior parasegment expression [21].

Finally, note that the maximal expression levels of *wg* are written in terms of the parameters $\alpha_{\text{CI}wg}$ and $\alpha_{\text{WG}wg}$. From Eq. (54), there are several possible combinations of the step functions, each leading to a different value for wg_2. These possibilities are given by:

$$w = \frac{R_{\text{CI}}\alpha_{\text{CI}wg} + R_{\text{WG}}\alpha_{\text{WG}wg}}{1 + R_{\text{CI}}\alpha_{\text{CI}wg} + R_{\text{WG}}\alpha_{\text{WG}wg}}, \tag{12}$$

where $R_{\text{CI}}, R_{\text{WG}} \in [0, 1]$ reflect the possible values of the step functions. Two different pathways for *wingless* activation can be identified. Indeed, *wingless* can be activated by Cubitus only (in which case $R_{\text{CI}} > 0$, $R_{\text{WG}} = 0$), or by Wingless only ($R_{\text{CI}} = 0$, $R_{\text{WG}} > 0$), or by both Cubitus and Wingless ($R_{\text{CI}}, R_{\text{WG}} > 0$).

4 Missing link: *engrailed* regulation by Cubitus repressor

A first result from our model formulation is the explanation of a "missing link" in a first version of the model proposed by von Dassow et al. [3]. In this first version, *engrailed* was regulated only by EWG, and no feasible parameter sets were found. Indeed, below (Theorem 1) we prove that, *for any set of parameters*, the mechanism for *wingless* regulation generates a strong symmetry in the steady state expression of

external Wingless. This mechanism effectively prevents any asymmetry arising in *en* due to EWG only.

Theorem 1 *Assume* $wg^{WT} = (w_1, w_2, w_3, w_4)'$, *with* $0 \leq w_4 \leq \min\{w_1, w_3\} \leq \max\{w_1, w_3\} < w_2$. *Then, at steady state:*

$$EWG_{\underline{4}}^{WT} \leq \min\{EWG_{\underline{1}}^{WT}, EWG_{\underline{3}}^{WT}\} \leq \max\{EWG_{\underline{1}}^{WT}, EWG_{\underline{3}}^{WT}\} < EWG_{\underline{2}}^{WT}. \qquad (13)$$

The proof is based on the following Lemma which is shown in Appendix E.

Lemma 4.1 *Let* $wg = (wg_1, wg_2, wg_3, wg_4)$. *There exist constants* $\beta_{\max} > \beta_{\mathrm{med}} > \beta_{\min} > 0$ *and* $\gamma_{\max} > \gamma_{\mathrm{med}} > \gamma_{\min} > 0$ *such that:*

$$EWG_1 = wg_1 \beta_{\max} + (wg_2 + wg_4)\beta_{\mathrm{med}} + wg_3 \beta_{\min},$$
$$EWG_2 = wg_2 \beta_{\max} + (wg_1 + wg_3)\beta_{\mathrm{med}} + wg_4 \beta_{\min},$$
$$EWG_3 = wg_3 \beta_{\max} + (wg_2 + wg_4)\beta_{\mathrm{med}} + wg_1 \beta_{\min},$$
$$EWG_4 = wg_4 \beta_{\max} + (wg_1 + wg_3)\beta_{\mathrm{med}} + wg_2 \beta_{\min}.$$

and

$$IWG_1 = wg_1 \gamma_{\max} + (wg_2 + wg_4)\gamma_{\mathrm{med}} + wg_3 \gamma_{\min},$$
$$IWG_2 = wg_2 \gamma_{\max} + (wg_1 + wg_3)\gamma_{\mathrm{med}} + wg_4 \gamma_{\min},$$
$$IWG_3 = wg_3 \gamma_{\max} + (wg_2 + wg_4)\gamma_{\mathrm{med}} + wg_1 \gamma_{\min},$$
$$IWG_4 = wg_4 \gamma_{\max} + (wg_1 + wg_3)\gamma_{\mathrm{med}} + wg_2 \gamma_{\min}.$$

Now, consider the steady state equation that would result if no dependence of *engrailed* on CN is assumed in Eq. (52):

$$en_i^{WT} = \theta^+ (EWG_{\underline{i}}^{WT}, \kappa_{WGen})$$

Compare to states in $\mathcal{W}$:

$$en_3 = N_3 \quad \text{and} \quad en_i = 0, \quad \text{for } i = 1, 2, 4.$$

Then, from the definition of θ^+, for consistency in our model it is necessary that:

$$EWG_{\underline{i}}^{WT} \leq \kappa_{WGen}, \quad \text{for } i = 1, 2, 4$$
$$EWG_{\underline{3}}^{WT} \geq \kappa_{WGen}.$$

However, by (13), the inequalities for $i = 2$ (and possibly $i = 1$) and $i = 3$ are incompatible. This means that, due to the symmetry in Wingless distribution, such a simple regulation of *en can never lead to the segment polarity pattern*. Thus *engrailed* requires regulation by some other factor, in this case repression by the Cubitus protein

(CN), as in (52). In order to obtain repression of *en* in the second cell, recalling (11) one can now ask:

$$\text{EWG}_{\underline{1}}^{\text{WT}} \leq \kappa_{\text{WGen}} \text{ or } \text{CN}_1^{\text{WT}} \geq \kappa_{\text{CNen}},$$
$$\text{CN}_2^{\text{WT}} \geq \kappa_{\text{CNen}},$$
$$\text{EWG}_{\underline{3}}^{\text{WT}} \geq \kappa_{\text{WGen}} \text{ and } \text{CN}_3^{\text{WT}} \leq \kappa_{\text{CNen}},$$
$$\text{EWG}_{\underline{4}}^{\text{WT}} \leq \kappa_{\text{WGen}} \text{ or } \text{CN}_4^{\text{WT}} \geq \kappa_{\text{CNen}},$$

that is, CN is responsible for repression in the second, and possibly in the first, cells. This means that, at steady state, CN must be expressed in both the first and second cells. This in turn requires the presence of Patched protein in both the first and second cells. On the other hand, from Appendix F, we know that a steady state $x \in \mathcal{W}$, implies $ptc_1^{\text{WT}} = \text{PTC}_1^{\text{WT}}$ and $ptc_3^{\text{WT}} = \text{PTC}_3^{\text{WT}} = 0$. While *patched* expression is typically weaker in the first than in second and fourth cells (see [3]), this shows that it is nevertheless necessary, that is, the segment polarity gene pattern obtains only when T_1 is above the expression threshold. The discussion on CN leads to the following conclusion:

Lemma 4.2 *Consider system* (1) *and assume that, at steady state, the system is in* $\mathcal{W}$, *that is* $ci^{\text{WT}} = (U_1, U_2, 0, U_4)'$ *and* $ptc^{\text{WT}} = (T_1, T_2, T_3, T_2)'$, *with* $U_{1,2,4} \geq \varepsilon$ *and* $T_3 < \varepsilon$. *Then* $PTC_{3,T}^{\text{WT}} = 0$ *and* $CI_3^{\text{WT}} = CN_3^{\text{WT}} = ci_3^{\text{WT}} = 0$ *and* $PTC_{2,T}^{\text{WT}} = PTC_{4,T}^{\text{WT}} > 0$. *Also* $PTC_{1,2,4}^{\text{WT}} \geq \kappa_{PTCCI}$ *and*

$$CN_i^{\text{WT}} = U_i \frac{Q_i H_{CI} C_{CI}}{1 + Q_i H_{CI} C_{CI}}, \quad i = 1, 2, 4, \quad CI_i^{\text{WT}} = U_i - CN_i = U_i \frac{1}{1 + Q_i H_{CI} C_{CI}}, \quad (14)$$

with

$$Q_i \in \begin{cases} \{1\}, & \text{if } PTC_{i,T} > \kappa_{PTCCI} \\ [0, 1], & \text{if } PTC_{i,T} = \kappa_{PTCCI}. \end{cases}$$

5 A cylindrical algebraic decomposition of the parameter space

The algebraic equations $f(x, p) = 0$ together with $x \in \mathcal{W}$ impose constraints on the set of good parameters (G), though not providing as yet explicit conditions on p. An explicit characterization of the parameters p may be obtained by calculating a cylindrical algebraic decomposition (CAD) of G: this is a special type of representation of G through a hierarchy of inequalities on the parameters. Suppose that a first family of parameters, say $\{p_1, \dots, p_{r_1}\}$ (with $1 \leq r_1 < r$) may take values in a product of intervals $L_1 \times \cdots \times L_{r_1}$ (where each interval may be open, closed or mixed). Then a CAD is defined as follows:

$$S_1 = L_1 \times \cdots \times L_{r_1} \subset \mathbb{R}^{r_1}$$
$$S_j = \{(\hat{p}, p_j) \in \mathbb{R}^j : \hat{p} = (p_1, \dots, p_{j-1})' \in S_{j-1}, \ f_j(\hat{p}) \prec p_j \prec g_j(\hat{p})\} \subset \mathbb{R}^j \quad (15)$$

for $j = r_1 + 1, \ldots, r$, where $f_j, g_j : S_{j-1} \to \mathbb{R}_{\geq 0}$ are continuous functions such that $f_j(\hat{p}) \leq g_j(\hat{p})$ for all $\hat{p} \in \mathbb{R}^{j-1}$, the symbol $\prec$ denotes either $<$ or $\leq$, and $S_r = G$.

Computing the cylindrical algebraic decomposition of a set is a complex problem, but various standard algorithms are available [22,23]. Several software packages have been developed, for instance QEPAD [24], (based in [25]) and in Mathematica [26]. See also [27] for an overview of available software, current applications, and many other related references. Common applications of CADs include computation of the controllable or reachabable sets in hybrid systems, see for instance [28,29], where the latter includes an application to a genetic network in the fly wing. Constructing a CAD involves the use of symbolic computation and, while various improvements have been achieved, it still is a time consuming problem. For instance, the estimated maximum time for the algorithm [22] is dominated by "$2^{2^{kN}}$", where N is the length of the input formula and $0 < k \leq 8$. Fortunately, in view of these computational complexity difficulties, in the present example it is relatively easy to directly compute a CAD without using general methods, and we will do so.

The computation of the feasible parameter set G for the segment polarity network is detailed in Appendix H. The CAD of G can be used to answer several questions regarding geometry and topology of the feasible parameter space. First, the volume of G can be estimated, relative to the unitary hypercube $[0, 1]^r$ ($r = 31$), as described in Sect. 6. Second, the topology of G can be analyzed, to find out its connectedness (e.g., simple-connectedness; or composed of various disconnected components). To summarize, we show that G can be written as a union of several regions:

$$G = G_{\mathrm{I}} \cup \cdots \cup G_{\mathrm{v}a} \cup G_{\mathrm{v}b} \cup \cdots \cup G_{\mathrm{VIII}a} \cup G_{\mathrm{VIII}b} \cup G_{\mathrm{Auto}}.$$

These 13 regions are all connected and, in particular, $G_{\mathrm{v}a}$ to $G_{\mathrm{VIII}b}$ are connecting faces and have a lower dimension (see Fig. 1e and Theorem 2, below).

Each of these regions has a CAD with nine levels, as listed next. The levels $S_1, \ldots, S_6$ are the same for all the regions G_k, $k \in \{\mathrm{I}, \ldots, \mathrm{VIII}b, \mathrm{Auto}\}$. The form of the last three levels depends on each region: S_7^k, S_8^k, S_9^k. At the base of the CADs, S_1 is a product of intervals for $r_1 = 23$ parameters (while $r = 31$), defined as follows:

$$S_1 : \begin{cases} p_{\mathrm{CI}} = (H_{\mathrm{CI}}, C_{\mathrm{CI}}, U_1, U_2, U_3, U_4), \in [5, 100] \times (0, 1] \times [\varepsilon, 1]^2 \times (0, 1] \times [\varepsilon, 1], \\ p_{\mathrm{PTC-HH}} = (H_{\mathrm{PTC}}, H_{\mathrm{HH}}, [\mathrm{PTC}]_0, [\mathrm{HH}]_0, r_{LM\mathrm{PTC}}, r_{LM\mathrm{HH}}, \kappa_{\mathrm{PTCHH}}) \in [5, 100]^2 \times (0, 1]^5, \\ p_{\mathrm{WG}} = (H_{\mathrm{WG}}, r_M, r_{LM}, r_{\mathrm{endo}}, r_{\mathrm{exo}}) \in [5, 100] \times (0, 1]^4, \\ \alpha_{\mathrm{CI}wg}, \alpha_{\mathrm{IWG}wg} \in [\frac{\varepsilon}{1-\varepsilon}, 10], \\ \kappa_{\mathrm{EN}ci}, \kappa_{\mathrm{EN}hh}, \kappa_{\mathrm{CN}hh} \in (0, 1]. \end{cases} \tag{16}$$

Levels S_2 to S_4 are characterized as follows:

$$S_2 = \left\{ (\hat{p}, \kappa_{\mathrm{PTCCI}}) : \hat{p} \in S_1, \ 0 < \kappa_{\mathrm{PTCCI}} \leq \min \left\{ F_{\mathrm{PTC}_{1,\mathrm{T}}}, F_{\mathrm{PTC}_{2,\mathrm{T}}} \right\} \right\}, \tag{17}$$

$$S_3 = \left\{ (\hat{p}, \kappa_{\mathrm{CN}ptc}) : \hat{p} \in S_2, \ \max \left\{ \frac{U_i Q_i H_{\mathrm{CI}} C_{\mathrm{CI}}}{1 + Q_i H_{\mathrm{CI}} C_{\mathrm{CI}}} \right\} \leq \kappa_{\mathrm{CN}ptc} \leq 1 \right\}, \tag{18}$$

$$S_4 = \left\{ (\hat{p}, \kappa_{\mathrm{CI}ptc}) : \hat{p} \in S_3, \ 0 < \kappa_{\mathrm{CI}ptc} \leq \min \left\{ \frac{U_i}{1 + Q_i H_{\mathrm{CI}} C_{\mathrm{CI}}} \right\} \right\}, \tag{19}$$

where $F_{\text{PTC}1,\text{T}}$, $F_{\text{PTC}2,\text{T}}$ are the solutions of the algebraic equations (58) for the set of parameters $\hat{p}$. Let $w_2 \in \{\frac{\alpha_{\text{CI}}}{1+\alpha_{\text{CI}}}, \frac{\alpha_{\text{WG}}}{1+\alpha_{\text{WG}}}, \frac{\alpha_{\text{WG}}+\alpha_{\text{CI}}}{1+\alpha_{\text{WG}}+\alpha_{\text{CI}}}\}$. Then levels S_5 and S_6 are characterized as:

$$S_5 = \left\{ (\hat{p}, \kappa_{\text{WG}en}) : \ \hat{p} \in S_4, 0 < \kappa_{\text{WG}en} \le w_2 \beta_{\text{med}} \right\}, \tag{20}$$

$$S_6 = \left\{ (\hat{p}, \kappa_{\text{CN}en}) : \ \hat{p} \in S_5, \ 0 < \kappa_{\text{CN}en} \le \min_{i=1,2} \left\{ \frac{U_i Q_i H_{\text{CI}} C_{\text{CI}}}{1 + Q_i H_{\text{CI}} C_{\text{CI}}} \right\}, \ \text{if } \kappa_{\text{WG}en} \in [w_2 \beta_{\text{min}}, w_2 \beta_{\text{med}}]; \right.$$
$$\left. \text{or } 0 < \kappa_{\text{CN}en} \le \min_{i=1,2,4} \left\{ \frac{U_i Q_i H_{\text{CI}} C_{\text{CI}}}{1 + Q_i H_{\text{CI}} C_{\text{CI}}} \right\}, \ \text{if } \kappa_{\text{WG}en} \in [0, w_2 \beta_{\text{min}}] \right\} \tag{21}$$

Finally, the last three levels have different expressions depending on the region of the parameter space:

$$S_7^k = \{(\hat{p}, \kappa_{\text{WG}wg}) : \ \hat{p} \in S_6, \ f_{\text{WG}wg}^k(\hat{p}) \prec \kappa_{\text{WG}wg} \prec g_{\text{WG}wg}^k(\hat{p})\}, \tag{22}$$

$$S_8^k = \{(\hat{p}, \kappa_{\text{CN}wg}) : \ \hat{p} \in S_7^k, \ f_{\text{CN}wg}^k(\hat{p}) \prec \kappa_{\text{CN}wg} \prec g_{\text{CN}wg}^k(\hat{p})\}, \tag{23}$$

$$S_9^k = \{(\hat{p}, \kappa_{\text{CI}wg}) : \ \hat{p} \in S_8^k, \ f_{\text{CI}wg}^k(\hat{p})\} \prec \kappa_{\text{CI}wg} \prec g_{\text{CI}wg}^k(\hat{p})\}, \tag{24}$$

where $k \in \{\text{I}, \ldots, \text{VIII}b, \text{Auto}\}$ and the functions f_j^k and g_j^k ($j \in \{\text{WG}wg, \text{CN}wg, \text{CI}wg\}$) are listed in Tables 4 and 5. These CADs have a biological interpretation (see discussion in Sect. 5.1): from Eqs. (52)–(63) subject to (4) and (5), several parameters are free to take any values, within physiological restrictions only—these form S_1. The parameters defined at the levels S_2 to S_6 have constraints which depend only on the family of parameters defined in S_1. The last levels, S_7^k to S_9^k define different regions of G, with the property that each region is associated to the activation of a particular biological pathway: G_{Auto} corresponds to activation of *wingless* on the second cell by the autocatalytic pathway only. In regions G_{I} to $G_{\text{VIII}b}$ the Cubitus pathway also promotes activation of *wingless*.

In the next lemma it is shown that each region G_k is topologically equivalent to a unitary closed hypercube, hence topologically trivial. However, some regions (G_{va} to $G_{\text{VIII}b}$) have a lower dimension. This is clear by observing Table 5: in each of these eight regions, either of the parameters $\kappa_{\text{CN}wg}$ or $\kappa_{\text{CI}wg}$ is a single point (as opposed to a non-trivial interval).

To simplify notation, for $i = 1, \ldots, 4$ define

$$\tilde{U}_i = U_i \frac{Q_i H_{\text{CI}} C_{\text{CI}}}{1 + Q_i H_{\text{CI}} C_{\text{CI}}}$$

and observe that $\text{CN}_i = \tilde{U}_i$ and $\text{CI}_i = U_i - \tilde{U}_i$.

Let $\prec$ denote either of the symbols $<$ or $\le$ and define

$$L_j = \{x \in \mathbb{R} : a_j \prec x \prec b_j\}.$$

Let $\mathcal{I}$ denote the unitary interval (open, closed or mixed):

$$\mathcal{I} = \{x \in \mathbb{R} : 0 \prec x \prec 1\}.$$

Theorem 2 *Consider the sets S_9^k, $k \in \{I, \ldots, VIIIb, Auto\}$, obtained from* (24). *Then* (*with $r = 31$*):

(i) S_9^k, $k = Auto, I, II, III, IV$ are homeomorphic to $\mathcal{I}^r$;

(ii) S_9^k, $k = Va, Vb, VIa, VIb, VIIa, VIIb, VIIIa, VIIIb$ are homeomorphic to $\mathcal{I}^{r-1} \times \{1\}$.

Proof Consider first case (i). To argue by induction, note that each L_j is clearly homeomorphic to the interval $\mathcal{I}$ (with the same open, closed or mixed boundaries as L_j), for $j = 1, \ldots, 23$. Since $a_j < b_j$ for all $j = 1, \ldots, 23$, simply consider the bijective function $\phi_j : L_j \to \mathcal{I}$ given by $\phi_j(p) = (b_j - p)/(b_j - a_j)$. Then the set $S_1 = L_1 \times \cdots \times L_{23}$ is homeomorphic to the product $\mathcal{I}^{23}$, by considering the bijective function $\varphi_1 : S_1 \to \mathcal{I}^{23}$ given by $\varphi_1(p_1, \ldots, p_{23}) = (\phi_1(p_1), \ldots, \phi_{23}(p_{23}))'$.

For $i \geq 2$, assume that S_{i-1} is homeomorphic to $\mathcal{I}^{i-1}$. Note that $f_i(p) < g_i(p)$ for all $i = 2, \ldots, 9$, for S_9^k with $k = $ Auto, I, II, III, IV. Next, define the following continuous function:

$$\varphi_i : S_{i-1} \times \mathcal{I} \to S_{i-1} \times \mathbb{R}, \quad \varphi_i(p, t) = (p, f_i(p) + t(g_i(p) - f_i(p))).$$

For each fixed p, $f_i(p) < g_i(p) + t(g_i(p) - f_i(p)) < g_i(p)$ for all $t \in \mathcal{I}$. Therefore, φ_i maps into S_i. On the other hand, since $g_i(p) - f_i(p) > 0$ for all $p \in S_{i-1}$, φ_i has an inverse function defined on S_i and continuous, given by:

$$\varphi_i^{-1} : S_i \to S_{i-1} \times \mathcal{I}, \quad \varphi_i^{-1}(p, y) = \left(p, \frac{y - f_i(y)}{g_i(p) - f_i(p)} \right).$$

So S_i is homeomorphic to $S_{i-1} \times \mathcal{I}$, and therefore, by inductive hypothesis, to $\mathcal{I}^i$.

Next, consider case (ii). From Table 5 it is clear that, in regions G_{va} to G_{VIIIb}, *exactly one* of the parameters κ_{CNwg} or κ_{Clwg} has a single point as an interval. So, the previous argument is valid up to S_{r-1} and then the last parameter is a point. This finishes the proof.   □

5.1 Two wingless mRNA activation pathways

Following the model of von Dassow et al., there are two possible parallel pathways for *wingless* activation: either by the Cubitus interruptus protein (CI), or through auto-activation; both pathways could be simultaneously activating *wingless* production. Since the activation constants α_{Clwg} and α_{WGwg}, are free parameters, in each of the three cases wg_2^{WT} will have a different ON level as calculated from (12). Computation of EWG and IWG depends on wg_2^{WT}, so each of these three cases must be separately analyzed for feasibility. For both pathways, exact analytic computation of $PTC_{i,j}$ and $HH_{i,j}$ ($i, j = 1, \ldots, 4$) is also carried out (see Appendix F). When CI and CN contribute to regulate *wingless* expression, it is easy to see from (5), (14) and (54) that:

$$U_i \frac{1}{1 + Q_i H_{CI} C_{CI}} \leq \kappa_{Clwg} \quad \text{or} \quad U_i \frac{Q_i H_{CI} C_{CI}}{1 + Q_i H_{CI} C_{CI}} \geq \kappa_{CNwg}, \qquad (25)$$

for $i = 1, 3, 4$, and

$$U_2 \frac{1}{1 + Q_2 H_{\mathrm{CI}} C_{\mathrm{CI}}} \geq \kappa_{\mathrm{CIwg}} \quad \text{and} \quad U_2 \frac{Q_2 H_{\mathrm{CI}} C_{\mathrm{CI}}}{1 + Q_2 H_{\mathrm{CI}} C_{\mathrm{CI}}} \leq \kappa_{\mathrm{CNwg}}. \tag{26}$$

From observation of (25) and (26) it is clear that the situations $\tilde{U}_2 = \tilde{U}_1$ or $\tilde{U}_2 = \tilde{U}_4$ define some critical regions. To see this, for simplicity consider $Q_i = 1$ (which is true for many parameter sets, i.e., $\kappa_{\mathrm{PTCCI}} < \min\{F_{\mathrm{PTC1,T}}, F_{\mathrm{PTC2,T}}\}$). Then $\tilde{U}_2 = \tilde{U}_1$ is compatible with the wild type pattern only when $\kappa_{\mathrm{CIwg}} = U_1 - \tilde{U}_1 = U_2 - \tilde{U}_2$ or $\kappa_{\mathrm{CNwg}} = \tilde{U}_1 = \tilde{U}_2$. Moreover, recalling the definition of step function, it follows that in this case $\theta^+(\mathrm{CI}_2 \theta^-(\mathrm{CN}_2, \kappa_{\mathrm{CNwg}}), \kappa_{\mathrm{CIwg}}) = [0, 1]$ and wg may in fact be either activated or not in cell 2. The set G can thus be partitioned into four "strictly feasible" components, divided by the critical hyperplanes $\tilde{U}_2 = \tilde{U}_1$ or $\tilde{U}_2 = \tilde{U}_4$ (Fig. 2). Note that, for parameters belonging to these hyperplanes: $wg_2 = \frac{R_{CI}\alpha_{CI} + R_{WG}\alpha_{WG}}{1 + R_{CI}\alpha_{CI} + R_{WG}\alpha_{WG}}$ where R_{CI} is any number in the interval $[0, 1]$. Thus there are multiple possible steady states, and some of these may not provide the right phenotype. These hyperplanes correspond, in fact, to regions G_V to G_{VIII}.

When only the wingless auto-activation pathway contributes to wingless activation, the necessary conditions are (when $Q_i = 1$):

$$\left(U_2 \frac{1}{1 + Q_2 H_{\mathrm{CI}} C_{\mathrm{CI}}} < \kappa_{\mathrm{CIwg}} \quad \text{or} \quad U_2 \frac{Q_2 H_{\mathrm{CI}} C_{\mathrm{CI}}}{1 + Q_2 H_{\mathrm{CI}} C_{\mathrm{CI}}} > \kappa_{\mathrm{CNwg}} \right) \quad \text{and} \quad \mathrm{IWG}_2 \geq \kappa_{\mathrm{WGwg}}. \tag{27}$$

Comparing (26) and (27) it is not surprising that, for each triple $(\tilde{U}_1, \tilde{U}_2, \tilde{U}_4)$, κ_{CIwg} and κ_{CNwg} belong to complementary intervals, since they define whether or not the CI/CN pathway is active. The projection on the $(\kappa_{\mathrm{CIwg}}, \kappa_{\mathrm{CNwg}}, \kappa_{\mathrm{WGwg}})$-dimensions, shown
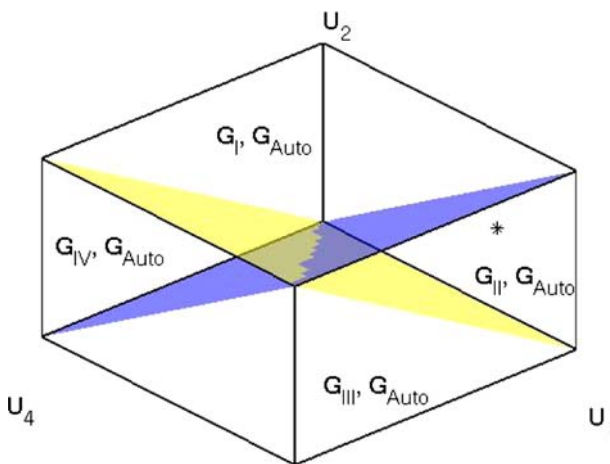
Fig. 2 Projection of set G into the (U_1, U_2, U_4) space (case $Q_i = 1$, $i = 1, 2, 4$). The critical hyperplanes $U_2 = U_4$ (*yellow/light grey*) and $U_2 = U_1$ (*blue/dark grey*) define four strictly feasible components
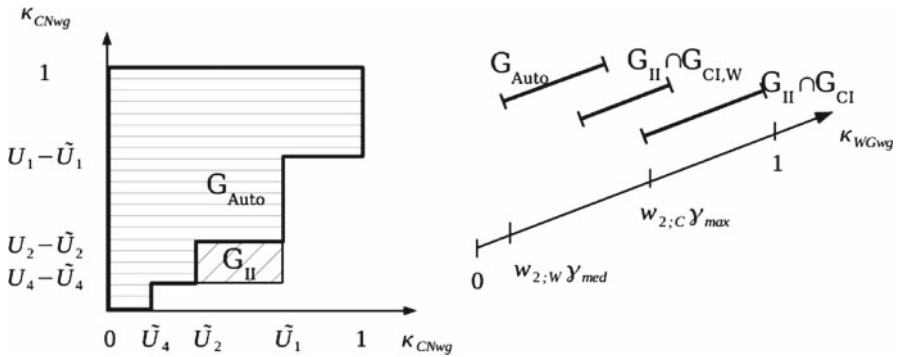
Fig. 3 Projection of G on the space $(\kappa_{CIwg}, \kappa_{CNwg}, \kappa_{WGwg})$, of the fibre over the point represented by "∗" in Fig. 2. This point corresponds to choosing values for (U_1, U_2, U_4) in region G_{II}. Depending on the choice of parameters S_1, the interval for κ_{WGwg} in G_{Auto} may or may not intersect the other two. The values $w_{2;\cdot}$ are defined in Table 4

in Fig. 3, compares the regions where CI/CN is active (G_{II}) or only WG is active (G_{Auto}), both polyhedrons.

6 Geometry, volume and the second missing link

From the CAD (16)–(24) it is very easy to compute the (relative) volume of G. Following a Monte Carlo approach, the free parameters (16) and also (17)–(19) are chosen first, from a uniform distribution in their respective intervals. Then the quintuple of parameters κ_{WGen}, κ_{CNen}, κ_{CIwg}, κ_{CNwg}, and κ_{WGwg} are randomly chosen (from a uniform distribution) in the interval $[0, 1]$. It is then checked whether the whole parameter set falls inside or outside G. If the parameter set falls inside G, we also check which *wingless* activation pathways are compatible, as well as the region (U_1, U_2, U_4). This Monte Carlo approach provides an estimate of the volume of G, when projected into the $(\kappa_{CNen}, \kappa_{WGen}, \kappa_{CIwg}, \kappa_{CNwg}, \kappa_{WGwg})$ dimensions. In addition, we also obtain an estimate of the fraction of the feasible parameter sets that correspond to either of the *wingless* activation pathways (Table 1).

The volume of this five-dimensional cube occupied by feasible parameter sets is only about 0.3%. Interestingly, we also found that the vast majority of the feasible

Table 1 Relative volume of G

Region	Volume
G_{Auto}	322×10^{-5}
G_{CI}	8.5×10^{-5}
$G_{CI,WG}$	1.5×10^{-5}

Fraction of G corresponding to each of the three *wingless* activation pathways: auto-regulation only (G_{Auto}), cubitus regulation only (G_{CI}), and both cubitus and wingless regulation ($G_{CI,WG}$). $G_{CI} \cup G_{CI,WG} = G_I \cup \cdots \cup G_{VIIIb}$. Total number of parameter sets generated: 1×10^7. Number of feasible parameter sets: 33276

parameter space corresponds to auto-regulation of wingless. As illustrated by the polyhedrons in Fig. 3, region G_{Auto} is much larger than the others. Here, regions G_{I} to $G_{\text{VIII}b}$ are re-grouped according to the biological pathway, following the indications in Tables 3 and 4. Region G_{CI} corresponds to wingless mRNA regulation by cubitus only, and region $G_{\text{CI,WG}}$ corresponds to regulation by both cubitus and wingless proteins. We have: $G_{\text{CI}} \cup G_{\text{CI,WG}} = G_{\text{I}} \cup \cdots \cup G_{\text{VIII}b}$, where each G_i intersects G_{CI} and $G_{\text{CI,WG}}$.

The large difference observed between G_{CI}, $G_{\text{CI,WG}}$ and G_{Auto} explains the second "missing link" in the first version of von Dassow et al. model, namely the *wingless* autocatalytic activation. Note that the presence of this link greatly increases the total volume of the feasible parameter space: in fact the region G_{Auto} is 96% of the total feasible volume.

6.1 Geometry: parameter distributions

To further analyze the geometry of the feasible parameter space, one may ask how the parameters are distributed in their intervals. For instance, is each parameter p_i more likely to attain high or low values more frequently, and can a specific "tendency" for each parameter p_i be identified. An answer to this question is obtained by computing the marginal distribution of each parameter from a family of randomly generated parameters in the full parameter space G. Taking all the parameter sets generated previously to compute the relative volume of G, and computing a histogram for each parameter, the result shown on Fig. 4 is obtained. As expected, many parameters have a uniform distribution, as their values do not influence the final outcome of the network in any particular way (for instance, most half-lives and diffusion-related parameters). Other parameters exhibit a marked tendency for higher (e.g., $\kappa_{\text{CN}ptc}$), medium (e.g., $\kappa_{\text{WG}wg}$) or lower (e.g., $\kappa_{\text{CI}ptc}$) values. All the parameters that exhibit a marked tendency are listed in Table 2, and classified according to their function in the network: for instance, $\kappa_{\text{CN}ptc}$ represents the repression of *ptc* by CN, and therefore, high values of $\kappa_{\text{CN}ptc}$ correspond to a weak repression.

A very similar analysis was performed by von Dassow and Odell [20], who also plotted the distribution of their family of feasible parameters to determine possible constraints for each parameter. Overall, our results agree very well with those of von Dassow and Odell: most tendencies found by these authors (see Fig. 6 and Table 1 of [20]) are confirmed by our parameter analysis. There are only six exceptions, where our analysis showed no tendency (compare columns 3 and 4 of Table 2), suggesting that these five parameters can, in fact, take values in a larger set, implying that the parameter space is larger than estimated in [20]. From these exceptions, $\kappa_{\text{EN}ci}$, $\kappa_{\text{EN}hh}$, $\kappa_{\text{CN}hh}$, and $r_{\text{endo WG}}$ all belong to the group of parameters which can be freely chosen. The other parameters are $\kappa_{\text{CN}wg}$, $\kappa_{\text{CI}wg}$, which depend on the U_i regions, and again our analysis shows that this pair has no preferred tendency.

A more detailed examination of the conditions on $\kappa_{\text{CI}wg}$ and $\kappa_{\text{CN}wg}$ turns out to be very illuminating. First, note that $\kappa_{\text{CI}wg}$ and $\kappa_{\text{CN}wg}$ actually define the pathway through which *wingless* is activated. That is, in each of the regions G_{Auto}, G_{CI} or $G_{\text{CI,WG}}$, $\kappa_{\text{CI}wg}$ and $\kappa_{\text{CN}wg}$ belong to distinct intervals as a function of U_i. Thus, it may be expected that the distribution of these parameters varies in each region. By plotting the histograms
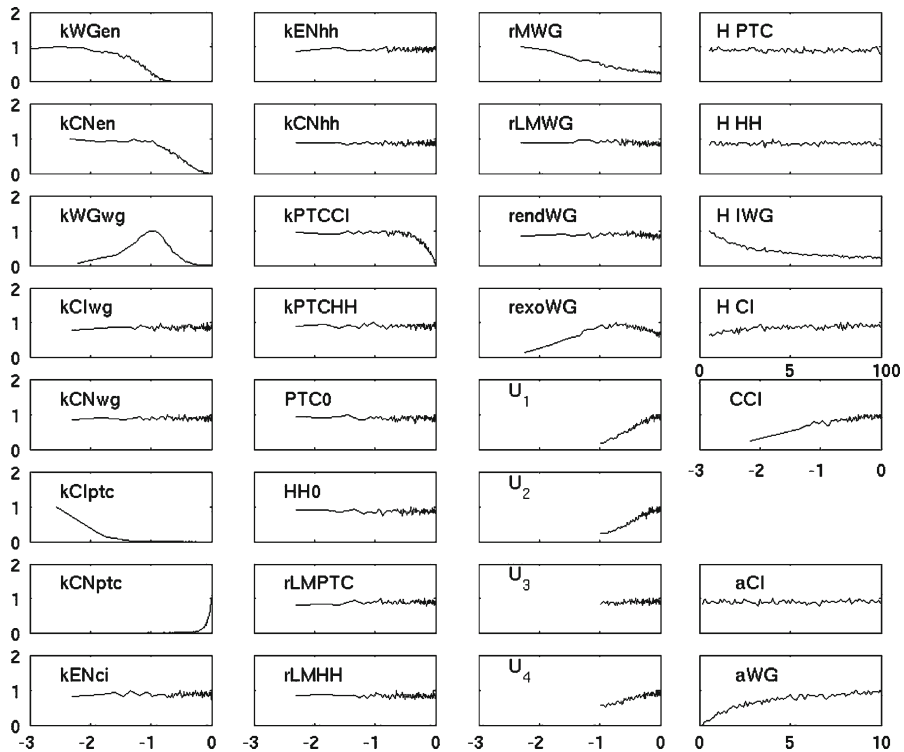
Fig. 4 Parameter histograms out of 33276 parameter sets (refer to model equations for explanation of parameters). The notation and scales follow those of Fig. 6 in [20]. In the y-axis, the histograms are all normalized to their maximal value. The half-lifes (denoted Hx) range between 5 and 100 mins in a linear scale. The coefficients aCIwg and aWGwg range between $\varepsilon/(1-\varepsilon) = 1/9$ and 10.0 also in a linear scale. All other parameters range between 10^{-3} and 1, and shown in $\log_{10}$ scale

for κ_{CIwg} and κ_{CNwg} for each region alone (Fig. 5), we note that these show a marked tendency only *outside* region G_{Auto}, for low κ_{CIwg} and high κ_{CNwg}. The tendency of κ_{CIwg} and κ_{CNwg} outside G_{Auto} is, however, the opposite of that observed by von Dassow and Odell, a fact that can be explained once again by the "second missing link". Since the volume of G_{Auto} is about 96% of G, it dominates the overall tendency. Indeed, since all feasible parameter sets in [3,20] were found only after adding the autocatalytic *wingless* activation link, it can be inferred that those parameters belong to region G_{Auto}.

7 Discussion and conclusions

Analysis of the feasible parameter set, by estimating its volume, identifying connected components, and studying its geometric properties, are valuable tools for establishing and quantifying robustness in regulatory networks. The concept of robustness, in the sense that the system's regulatory functions should operate correctly under a variety of situations, is closely related to the parameter space and the effect of parameter perturbations. In this context, our analysis of the model of the segment polarity

Table 2 Comparison between the constraints identified by von Dassow and Odell [20], and the exact constraints given by the regions defined above

Parameter	Description	Tendency [20, Table 1]	Tendency (within G)	Tendency ($G_{CI} + G_{CI,WG}$)
κ_{WGen}	WG activation of en	Moderate	Moderate	
κ_{CNen}	CN repression of en	Strong	Strong	
κ_{WGwg}	WG autoactivation	Moderate	Moderate	
κ_{CIwg}	CI activation of wg	Weak	—	Strong
κ_{CNwg}	CN repression of wg	Strong	—	Weak
κ_{CIptc}	CI activation of ptc	Strong	Strong	
κ_{CNptc}	CN repression of ptc	Weak	Weak	
κ_{ENci}	EN repression of ci	Moderate	—	
κ_{PTCCI}	PTC stimulation of CI cleavage	Strong	Strong	
κ_{ENhh}	EN activation of hh	Weak	—	
κ_{CNhh}	CN repression of hh	Strong	—	
C_{CI}	Maximal cleavage rate of CI	Rapid	Rapid	
H_{IWG}	Half-life of intracellular WG	Short	Short	
$r_{endo\ WG}$	Rate of WG endocytosis	Slow	—	
$r_{exo\ WG}$	Rate of WG exocytosis	Moderately slow	Moderately fast	
$r_{MxferWG}$	Rate of WG cell-to-cell exchange	Slow	Slow	
α_{WGwg}	Maximal WG autocatalytic rate	—	Moderately rapid	

Total number of parameters generated in G: 33276
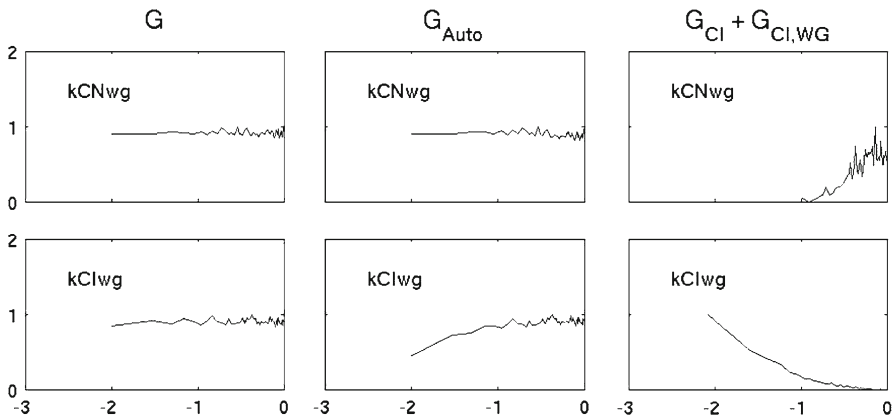
Fig. 5 Comparison of histograms for the pair κ_{CIwg}, κ_{CNwg}, in the whole feasible parameter space (G) and in the regions corresponding to the auto-catalytic pathway (G_{Auto}), or the cubitus pathway ($G_{CI} + G_{CI,WG}$). The x-axis is shown in $\log_{10}$ scale

network proposed in [3] shows that its feasible parameter space is composed of a single connected component, indicating a high robustness. However, we have found one topological and one geometric property which may contribute to lower robustness. First, there are two distinct regions in the parameter space (which correspond

to two adjacent "cubes" , see Fig. 3) associated with two different biological pathways: either auto-catalytic activation of *wingless* or activation by cubitus proteins only. Second, we have identified two lower dimensional planes of critical parameters ($\tilde{U}_2 = \tilde{U}_1$ and $\tilde{U}_2 = \tilde{U}_4$), where the model may fail to generate the wild type pattern. Since they form a lower dimensional space, these critical parameters are not likely to be an operating mode of the network. Nevertheless, the critical planes separate part of the feasible parameter space into four regions. An implication of this topological characterization is a diminished capacity of the network to respond well to environmental perturbations. Random fluctuations may drive the system through one of the critical planes, and possibly lead to a break down of the network or a different phenotype.

The reason why the planes $\tilde{U}_2 = \tilde{U}_1$ and $\tilde{U}_2 = \tilde{U}_4$ are critical can be traced in large part to an incompatibility of cubitus repression functions in the second cell: CN_2 should be present to repress *engrailed* expression, but should be absent to enhance CI_2 activation of *wingless*. To increase the network's robustness to environmental fluctuations, the segment polarity model should account for *engrailed* regulation by other factor than cubitus. One possibility is to include regulation by pair-rule gene products, such as sloppy paired, as explored both in [8,9]. An external factor, again possibly from the pair-rule genes, will also play a major role in establishing asymmetry in the *cubitus* levels (U_i). These contribute to a larger admissible parameter space, and together with an improved *engrailed* regulation, will greatly enhance robustness of the segment polarity network in maintaining its pattern. An extension of the current analysis including the regulation by sloppy paired can be found in [15].

Comparing the volume estimates for the regions G_{Auto} and G_{CI} or $G_{\text{CI,WG}}$ shows that the first accounts for about 96% of the total feasible volume. Thus it seems much more likely that wild type expression in this model of the segment polarity network is achieved through the wingless auto-activation pathway. In the absence of the auto-activation link, von Dassow et al. failed to observe any feasible parameter set in their numerical experiments. However, as soon as the auto-activation pathway was added (the second "missing link" in the model [3]), immediately a significant percentage of feasible parameter sets were observed. This is not surprising, as elucidated by our analysis: while *wingless* auto-activation is not strictly necessary to establishing the segment polarity genes pattern, it does greatly increase the probability that the pattern is achieved, by increasing the volume of the feasible parameter space. At the same time, the parameter histogram for the activity threshold κ_{WGwg} is very sharp, when compared with the other parameters (and our results are in clear agreement with the original study by von Dassow et al. [20]). This indicates that fine tuning of κ_{WGwg} is essential to maintenance of the asymmetric *wg* pattern. Note that (cf. Theorem 1) wingless protein concentration is only sligthly higher in the *wg*-expressing cell (2nd cell) than in its two immediate neighbours (1st and 3rd cells). Thus, fine tuning of κ_{WGwg} is necessary to promote auto-activation in the 2nd cell but prevent auto-activation in the 1st and 3rd cells.

The analysis developed in this paper can be applied to other systems and regulatory networks, to systematically characterize and explore the admissible space of parameters, its topology and geometry. The method presented here assumes there is a (fixed) set of target states or "pattern" ($\mathcal{W}$) to be reproduced (or avoided) by the

system, typically a desired steady state of the system. This pattern should also satisfy a family of algebraic equations ($x = f(x; p)$), on the variables and parameters of the system. These equations can be those characterizing the system at steady state for instance, but can also include other constraints as long as they are written in this form. To obtain a family of equations that is easier to deal with, the functions $f(x; p)$ may be simplified using reasonable approximations. For instance, sigmoidal type functions may be approximated by piecewise constant step functions. These equations are then symbolically solved with respect to the parameters. As a result, one obtains a family of inequalities characterizing the set of parameters *compatible* with the desired pattern and constraints. It is not guaranteed that an nonempty set of compatible parameters exists, as this depends on the constraints. Computation of a cylindrical algebraic decomposition is the main difficulty of this method. In general one may expect that it will work best with smaller/medium systems (on the order of 10–20 variables).

Our results emphasize that robustness of a regulatory module should not be measured simply as a function of the volume of its admissible parameter space. The geometry (for instance, convexity or existence of sharp points) and topology (connectedness) of the parameter space play fundamental roles in measuring robustness. These provide reliable information on how the network's interactions contribute to its robustness or fragility, and serve as measures to classify robust regulatory modules.

Appendix A: Notation

The original model can be found in [3,20]. In order to make our work more clear, we include the notation as well as the original equations below. Without loss of generality (the geometry remains unchanged), each cell is assumed to have four faces (Fig. 6), rather than six as in the original model [3]. The model reproduces a parasegment of four cells and uses repetition of this group of four cells to reproduce the embryo's anterior/posterior axis (A/P axis in Fig. 6), and the circular ventral/dorsal axis (V/D axis in Fig. 6). Because intercellular diffusion is only considered along the A/P axis (left/right), and because cells repeat in the orthogonal V/D direction (up/down), it is indeed equivalent to consider symmetric four-sided or six-sided hexagonal cells.

A saturation function, and its horizontal reflexion, are introduced:

$$\phi(X, \kappa, \nu) = \frac{X^\nu}{\kappa^\nu + X^\nu},$$

$$\psi(X, \kappa, \nu) = 1 - \phi(X, \kappa, \nu).$$
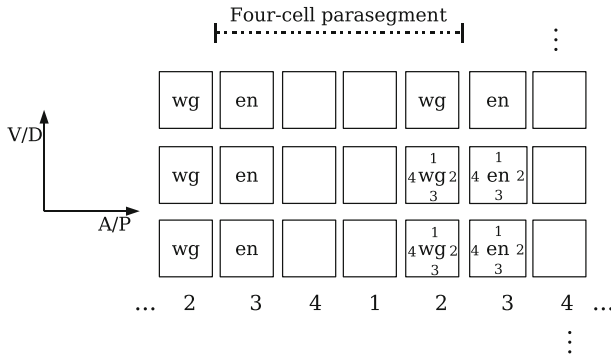
Fig. 6 Four cells in a parasegment, with periodic boundary conditions in both dimensions. Each cell has four membranes. The relative values of Wingless in each cell (EWG_i) are shown

The subscripted variables are as follows:

$$X_i = \text{concentration of species } X \text{ on cell } i \text{ (when homogeneous}$$
$$\text{throughout the cell)},$$

$$X_{i,j} = \text{concentration of species } X \text{ on cell } i, \text{ at face } j,$$

$$\kappa_{XY} = \text{threshold for activation of species } Y, \text{ induced by species } X,$$

$$n(i,j) = \text{index of neighbor to cell } i, \text{ at face } j,$$

$$X_{n(i,j),j+2} = \text{concentration of species } X \text{ on cell face apposite to } i, j,$$

$$X_{i,\text{T}} = \sum_{j=1}^{4} X_{i,j} = \text{total concentration of species } X \text{ on cell } i,$$

$$X_{\underline{i}} = \sum_{j=1}^{4} X_{n(i,j),j+2} = \text{total concentration of species } X \text{ presented to}$$

$$\text{cell } i \text{ by its neighbors.}$$

Appendix B: Original equations

From [3,20], the model equations are:

$$\frac{den_i}{dt} = \frac{1}{H_{en}}\left(\phi(EWG_{\underline{i}}\psi(CN_i, \kappa_{CNen}, \nu_{CNen}), \kappa_{WGen}, \nu_{WGen}) - en_i\right) \tag{28}$$

$$\frac{dEN_i}{dt} = \frac{1}{H_{EN}}(en_i - EN_i) \tag{29}$$

$$\frac{dwg_i}{dt} = \frac{1}{H_{wg}}\left(\frac{\alpha_{CIwg}\phi(CI_i\psi(CN_i, \kappa_{CNwg}, \nu_{CNwg}), \kappa_{CIwg}, \nu_{CIwg}) + \alpha_{WGwg}\phi(IWG_i, \kappa_{WGwg}, \nu_{WGwg})}{1 + \alpha_{CIwg}\phi(CI_i\psi(CN_i, \kappa_{CNwg}, \nu_{CNwg}), \kappa_{CIwg}, \nu_{CIwg}) + \alpha_{WGwg}\phi(IWG_i, \kappa_{WGwg}, \nu_{WGwg})} - wg_i\right) \tag{30}$$

$$\frac{d\text{IWG}_i}{dt} = \frac{1}{H_{\text{WG}}}\left(wg_i - \text{IWG}_i + r_{\text{endo}}H_{\text{IWG}}\text{EWG}_{i,\text{T}} - H_{\text{WG}}r_{\text{exo}}\text{IWG}_i\right) \tag{31}$$

$$\frac{d\text{EWG}_{i,j}}{dt} = \frac{1}{4}r_{\text{exo}}\text{IWG}_i - r_{\text{endo}}\text{EWG}_{i,j} + r_M(\text{EWG}_{n(i,j),j+2} - \text{EWG}_{i,j})$$

$$+ r_{LM}(\text{EWG}_{i,j-1} + \text{EWG}_{i,j+1} - 2\text{EWG}_{i,j}) - \frac{\text{EWG}_{i,j}}{H_{\text{WG}}} \tag{32}$$

$$\frac{dptc_i}{dt} = \frac{1}{H_{ptc}}\left(\phi(\text{CI}_i\psi(\text{CN}_i, \kappa_{\text{CN}ptc}, \nu_{\text{CN}ptc}), \kappa_{\text{CI}ptc}, \nu_{\text{CI}ptc}) - ptc_i\right) \tag{33}$$

$$\frac{d\text{PTC}_{i,j}}{dt} = \frac{1}{H_{\text{PTC}}}\left(\frac{1}{4}ptc_i - \text{PTC}_{i,j} - \kappa_{\text{PTCHH}}H_{\text{PTC}}[\text{HH}]_0\text{HH}_{n(i,j),j+2}\text{PTC}_{i,j}\right)$$

$$+ r_{LM\text{PTC}}(\text{PTC}_{i,j-1} + \text{PTC}_{i,j+1} - 2\text{PTC}_{i,j}) \tag{34}$$

$$\frac{dci_i}{dt} = \frac{1}{H_{ci}}\left(\phi(B_i\psi(\text{EN}_i, \kappa_{\text{EN}ci}, \nu_{\text{EN}ci}), \kappa_{\text{B}ci}, \nu_{\text{B}ci}) - ci_i\right) \tag{35}$$

$$\frac{d\text{CI}_i}{dt} = \frac{1}{H_{\text{CI}}}\left(ci_i - \text{CI}_i - H_{\text{CI}}C_{\text{CI}}\text{CI}_i\phi(\text{PTC}_{i,\text{T}}, \kappa_{\text{PTCCI}}, \nu_{\text{PTCCI}})\right) \tag{36}$$

$$\frac{d\text{CN}_i}{dt} = \frac{1}{H_{\text{CI}}}\left(H_{\text{CI}}C_{\text{CI}}\text{CI}_i\phi(\text{PTC}_{i,\text{T}}, \kappa_{\text{PTCCI}}, \nu_{\text{PTCCI}}) - \text{CN}_i\right) \tag{37}$$

$$\frac{dhh_i}{dt} = \frac{1}{H_{hh}}\left(\phi(\text{EN}_i\psi(\text{CN}_i, \kappa_{\text{CN}hh}, \nu_{\text{CN}hh}), \kappa_{\text{EN}hh}, \nu_{\text{EN}hh}) - hh_i\right) \tag{38}$$

$$\frac{d\text{HH}_{i,j}}{dt} = \frac{1}{H_{\text{HH}}}\left(\frac{1}{4}hh_i - \text{HH}_{i,j} - \kappa_{\text{PTCHH}}H_{\text{HH}}[\text{PTC}]_0\text{PTC}_{n(i,j),j+2}\text{HH}_{i,j}\right)$$

$$+ r_{LM\text{HH}}(\text{HH}_{i,j-1} + \text{HH}_{i,j+1} - 2\text{HH}_{i,j}) \tag{39}$$

Appendix C: Simplified model, for large ν

Using the approximations (10) and (11) the right-hand side of the von Dassow et al. is simplified as follows:

$$f_{en_i} = \frac{1}{H_{en}}\left(\theta^+(\text{EWG}_i\underline{\theta}^-(\text{CN}_i, \kappa_{\text{CN}en}), \kappa_{\text{WG}en}) - en_i\right) \tag{40}$$

$$f_{\text{EN}_i} = \frac{1}{H_{\text{EN}}}(en_i - \text{EN}_i) \tag{41}$$

$$f_{wg_i} = \frac{1}{H_{wg}}\left(\frac{\alpha_{\text{CI}wg}\theta^+(\text{CI}_i\theta^-(\text{CN}_i, \kappa_{\text{CN}wg}), \kappa_{\text{CI}wg}) + \alpha_{\text{WG}wg}\theta^+(\text{IWG}_i, \kappa_{\text{WG}wg})}{1 + \alpha_{\text{CI}wg}\theta^+(\text{CI}_i\theta^-(\text{CN}_i, \kappa_{\text{CN}wg}), \kappa_{\text{CI}wg}) + \alpha_{\text{WG}wg}\theta^+(\text{IWG}_i, \kappa_{\text{WG}wg})} - wg_i\right) \tag{42}$$

$$f_{\text{IWG}_i} = \frac{1}{H_{\text{WG}}}\left(wg_i - \text{IWG}_i + r_{\text{endo}}H_{\text{IWG}}\text{EWG}_{i,\text{T}} - H_{\text{WG}}r_{\text{exo}}\text{IWG}_i\right) \tag{43}$$

$$f_{\text{EWG}_{i,j}} = \frac{1}{4} r_{\text{exo}} \text{IWG}_i - r_{\text{endo}} \text{EWG}_{i,j} + r_M (\text{EWG}_{n(i,j),j+2} - \text{EWG}_{i,j})$$

$$+ r_{LM} (\text{EWG}_{i,j-1} + \text{EWG}_{i,j+1} - 2\text{EWG}_{i,j}) - \frac{\text{EWG}_{i,j}}{H_{\text{WG}}} \tag{44}$$

$$f_{ptc_i} = \frac{1}{H_{ptc}} \left(\theta^+ (\text{CI}_i \theta^- (\text{CN}_i, \kappa_{\text{CN}ptc}), \kappa_{\text{CI}ptc}) - ptc_i \right) \tag{45}$$

$$f_{\text{PTC}_{i,j}} = \frac{1}{H_{\text{PTC}}} \left(\frac{1}{4} ptc_i - \text{PTC}_{i,j} - \kappa_{\text{PTCHH}} H_{\text{PTC}} [\text{HH}]_0 \text{HH}_{n(i,j),j+2} \text{PTC}_{i,j} \right)$$

$$+ r_{LM\text{PTC}} (\text{PTC}_{i,j-1} + \text{PTC}_{i,j+1} - 2\text{PTC}_{i,j}) \tag{46}$$

$$f_{ci_i} = \frac{1}{H_{ci}} \left(U_i \theta^- (\text{EN}_i, \kappa_{\text{EN}ci}) - ci_i \right) \tag{47}$$

$$f_{\text{CI}_i} = \frac{1}{H_{\text{CI}}} \left(ci_i - \text{CI}_i - H_{\text{CI}} C_{\text{CI}} \text{CI}_i \theta^+ (\text{PTC}_{i,\text{T}}, \kappa_{\text{PTCCI}}) \right) \tag{48}$$

$$f_{\text{CN}_i} = \frac{1}{H_{\text{CI}}} \left(H_{\text{CI}} C_{\text{CI}} \text{CI}_i \theta^+ (\text{PTC}_{i,\text{T}}, \kappa_{\text{PTCCI}}) - \text{CN}_i \right) \tag{49}$$

$$f_{hh_i} = \frac{1}{H_{hh}} \left(\theta^+ (\text{EN}_i \theta^- (\text{CN}_i, \kappa_{\text{CN}hh}), \kappa_{\text{EN}hh}) - hh_i \right) \tag{50}$$

$$f_{\text{HH}_{i,j}} = \frac{1}{H_{\text{HH}}} \left(\frac{1}{4} hh_i - \text{HH}_{i,j} - \kappa_{\text{PTCHH}} H_{\text{HH}} [\text{PTC}]_0 \text{PTC}_{n(i,j),j+2} \text{HH}_{i,j} \right)$$

$$+ r_{LM\text{HH}} (\text{HH}_{i,j-1} + \text{HH}_{i,j+1} - 2\text{HH}_{i,j}). \tag{51}$$

To obtain Eq. (47) note that, in the original model of von Dassow et al., ci is written in terms of a constant forcing B_i:

$$ci_i = \theta^+ (B_i \theta^- (\text{EN}_i, \kappa_{\text{EN}ci}), \kappa_{\text{B}ci}),$$

where B_i is itself a parameter. Our definition of step function allows to merge the two parameters B_i and $\kappa_{\text{B}ci}$ into one single parameter U_i by letting

$$U_i \in \begin{cases} \{0\}, & B_i < \kappa_{\text{B}ci} \\ [0,1], & B_i = \kappa_{\text{B}ci} \\ \{1\}, & B_i > \kappa_{\text{B}ci}. \end{cases}$$

More generality is obtained by assuming that $B_i = \kappa_{\text{B}ci}$, and always allowing $U_i \in [0,1]$.

Appendix D: Steady state equations

Solving equations (28)–(39) at steady state $(dx/dt = f(x) = 0)$, and using the approximations (10), (11), yields the algebraic expressions:

$$en_i = \theta^+ (\text{EWG}_{\underline{i}} \theta^- (\text{CN}_i, \kappa_{\text{CN}en}), \kappa_{\text{WG}en}) \tag{52}$$

$$\text{EN}_i = en_i \tag{53}$$

$$wg_i = \frac{\alpha_{\text{CI}wg}\theta^+(\text{CI}_i\theta^-(\text{CN}_i, \kappa_{\text{CN}wg}), \kappa_{\text{CI}wg}) + \alpha_{\text{WG}wg}\theta^+(\text{IWG}_i, \kappa_{\text{WG}wg})}{1 + \alpha_{\text{CI}wg}\theta^+(\text{CI}_i\theta^-(\text{CN}_i, \kappa_{\text{CN}wg}), \kappa_{\text{CI}wg}) + \alpha_{\text{WG}wg}\theta^+(\text{IWG}_i, \kappa_{\text{WG}wg})} \tag{54}$$

$$\text{IWG}_i = \frac{H_{\text{IWG}}r_{\text{endo}}}{1 + H_{\text{IWG}}r_{\text{exo}}}\text{EWG}_{i,T} + \frac{1}{1 + H_{\text{IWG}}r_{\text{exo}}}wg_i \tag{55}$$

$$M\,\text{EWG} = -\frac{1}{4}\frac{r_{\text{exo}}}{1 + H_{\text{IWG}}r_{\text{exo}}}\widetilde{wg} \tag{56}$$

$$ptc_i = \theta^+(\text{CI}_i\theta^-(\text{CN}_i, \kappa_{\text{CN}ptc}), \kappa_{\text{CI}ptc}) \tag{57}$$

$$\text{PTC}_{i,j} = \frac{1}{4}ptc_i - \kappa_{\text{PTCHH}}H_{\text{PTC}}[\text{HH}]_0\text{HH}_{n(i,j),j+2}\text{PTC}_{i,j}$$
$$+ r_{LM\text{PTC}}H_{\text{PTC}}(\text{PTC}_{i,j-1} + \text{PTC}_{i,j+1} - 2\text{PTC}_{i,j}) \tag{58}$$

$$ci_i = U_i\,\theta^-(\text{EN}_i, \kappa_{\text{EN}ci}) \tag{59}$$

$$\text{CI}_i = U_i\,\frac{1}{1 + H_{\text{CI}}C_{\text{CI}}\,\theta^+(\text{PTC}_{i,\text{T}}, \kappa_{\text{PTCCI}})}\,\theta^-(\text{EN}_i, \kappa_{\text{EN}ci}) \tag{60}$$

$$\text{CN}_i = U_i\,\frac{H_{\text{CI}}C_{\text{CI}}\,\theta^+(\text{PTC}_{i,\text{T}}, \kappa_{\text{PTCCI}})}{1 + H_{\text{CI}}C_{\text{CI}}\,\theta^+(\text{PTC}_{i,\text{T}}, \kappa_{\text{PTCCI}})}\,\theta^-(\text{EN}_i, \kappa_{\text{EN}ci}) \tag{61}$$

$$hh_i = \theta^+(\text{EN}_i\theta^-(\text{CN}_i, \kappa_{\text{CN}hh}), \kappa_{\text{EN}hh}) \tag{62}$$

$$\text{HH}_{i,j} = \frac{1}{4}hh_i - \kappa_{\text{PTCHH}}H_{\text{HH}}[\text{PTC}]_0\text{PTC}_{n(i,j),j+2}\text{HH}_{i,j}$$
$$+ r_{LM\text{HH}}H_{\text{HH}}(\text{HH}_{i,j-1} + \text{HH}_{i,j+1} - 2\text{HH}_{i,j}) \tag{63}$$

EWG is a vector in $\mathbb{R}^{16}$ with components:

$$\text{EWG} = (\text{EWG}_{1,1}, \text{EWG}_{1,2}, \text{EWG}_{1,3}, \text{EWG}_{1,4}, \text{EWG}_{2,1}, \text{EWG}_{2,2}, \text{EWG}_{2,3}, \text{EWG}_{2,4},$$
$$\text{EWG}_{3,1}, \text{EWG}_{3,2}, \text{EWG}_{3,3}, \text{EWG}_{3,4}, \text{EWG}_{4,1}, \text{EWG}_{4,2}, \text{EWG}_{4,3}, \text{EWG}_{4,4})'$$

$\widetilde{wg}$ is also a vector in $\mathbb{R}^{16}$, given by the following Kronecker tensor product

$$\widetilde{wg} = (wg_1, wg_2, wg_3, wg_4)' \times_{\text{kron}} (1, 1, 1, 1)'$$
$$= (wg_1, wg_1, wg_1, wg_1, wg_2, wg_2, wg_2, wg_2,$$
$$wg_3, wg_3, wg_3, wg_3, wg_4, wg_4, wg_4, wg_4)'.$$

Putting together the 16 equations (56), and substituting IWG_i by its steady state expression (55), it is not difficult to see that the matrix $M \in \mathbb{R}^{16} \times \mathbb{R}^{16}$ is composed of various 4×4 blocks, as follows:

$$M = \begin{pmatrix} E & F_{24} & 0 & F_{42} \\ F_{42} & E & F_{24} & 0 \\ 0 & F_{42} & E & F_{24v} \\ F_{24} & 0 & F_{42} & E \end{pmatrix} \tag{64}$$

where

$$E = \begin{pmatrix} -d & r_{LM} & r_M & r_{LM} \\ r_{LM} & -d & r_{LM} & 0 \\ r_M & r_{LM} & -d & r_{LM} \\ r_{LM} & 0 & r_{LM} & -d \end{pmatrix} + h \begin{pmatrix} 1 & 1 & 1 & 1 \\ 1 & 1 & 1 & 1 \\ 1 & 1 & 1 & 1 \\ 1 & 1 & 1 & 1 \end{pmatrix}$$

with

$$d = H_{\text{IWG}}^{-1} + r_{\text{endo}} + r_M + 2r_{LM},$$

$$h = \frac{1}{4} \frac{H_{\text{IWG}} \, r_{\text{exo}}}{1 + H_{\text{IWG}} r_{\text{exo}}} r_{\text{endo}}$$

$$F_{24} = \begin{pmatrix} 0 & 0 & 0 & 0 \\ 0 & 0 & 0 & r_M \\ 0 & 0 & 0 & 0 \\ 0 & 0 & 0 & 0 \end{pmatrix}, \quad F_{42} = F_{24}' = \begin{pmatrix} 0 & 0 & 0 & 0 \\ 0 & 0 & 0 & 0 \\ 0 & 0 & 0 & 0 \\ 0 & r_M & 0 & 0 \end{pmatrix}.$$

Note that the steady state equations for EN, IWG, EWG and PTC are algebraic, and in fact exact solutions can be computed from the steady state values of *wg* and *ptc*. These are discussed in more detail in the Appendices E and F.

Remark The parameters are as in [3], except U_i, which represent the maximal values of *ci*, in each cell. These take values in the interval [0, 1] and generalize the possible ON values of *ci* (see explanation in Appendix C).

Appendix E: Analytically solving Wingless levels

The steady states of Wingless proteins (55) and (56) are given directly by algebraic equations, depending only on wingless mRNA (wg_2) and diffusion parameters for intracellular (membrane-to-membrane) and intercellular communication. Consider Eq. (56): it is easy to see that M is in fact always invertible (if all parameters are positive). First note that the matrix is diagonally dominant, by adding up the entries in any column:

$$-\left(H_{\text{IWG}}^{-1} + r_{\text{endo}} + r_M + 2r_{LM} \right) + 2r_{LM} + r_M + 4h = -H_{\text{IWG}}^{-1} - r_{\text{endo}} \frac{1}{1 + H_{\text{IWG}} r_{\text{exo}}}$$

which is always a negative quantity. By Geršgorin's Theorem, all eigenvalues of M are contained in the disk centered at $-d + h$ with radius $2r_{LM} + r_M + 3h$, therefore all have negative real parts. Thus, the matrix M is symmetric and negative definite, and since the right-hand side vector is also non-positive, all solutions are real and positive, *whatever the choice of parameters*. As a fact, note that the vector $\vec{1} = (1, 1, \ldots, 1)' \in \mathbb{R}^{16}$ is an eigenvector of M, corresponding to the eigenvalue $\lambda_1 = -H_{\text{IWG}}^{-1} - r_{\text{endo}} \frac{1}{H_{\text{IWG}} + r_{\text{exo}}}$.

The solution of Eqs. (56) and (55) can be written in terms of $wg = (wg_1, wg_2, wg_3, wg_4)$ as described next.

Lemma E.1 *There exist constants $\beta_{\max} > \beta_{\text{med}} > \beta_{\min} > 0$ and $\gamma_{\max} > \gamma_{\text{med}} > \gamma_{\min} > 0$ such that*:

$$EWG_1 = wg_1 \beta_{\max} + (wg_2 + wg_4)\beta_{\text{med}} + wg_3 \beta_{\min},$$
$$EWG_2 = wg_2 \beta_{\max} + (wg_1 + wg_3)\beta_{\text{med}} + wg_4 \beta_{\min},$$
$$EWG_3 = wg_3 \beta_{\max} + (wg_2 + wg_4)\beta_{\text{med}} + wg_1 \beta_{\min},$$
$$EWG_4 = wg_4 \beta_{\max} + (wg_1 + wg_3)\beta_{\text{med}} + wg_2 \beta_{\min}.$$

and

$$IWG_1 = wg_1 \gamma_{\max} + (wg_2 + wg_4)\gamma_{\text{med}} + wg_3 \gamma_{\min},$$
$$IWG_2 = wg_2 \gamma_{\max} + (wg_1 + wg_3)\gamma_{\text{med}} + wg_4 \gamma_{\min},$$
$$IWG_3 = wg_3 \gamma_{\max} + (wg_2 + wg_4)\gamma_{\text{med}} + wg_1 \gamma_{\min},$$
$$IWG_4 = wg_4 \gamma_{\max} + (wg_1 + wg_3)\gamma_{\text{med}} + wg_2 \gamma_{\min}.$$

Proof Observe that (56) can be written:

$$\vec{E} = -\frac{1}{4} \frac{r_{\text{exo}}}{1 + H_{\text{IWG}} r_{\text{exo}}} M^{-1} \widetilde{wg}$$

$$= -wg_1 c M^{-1} \begin{pmatrix} \vec{1} \\ \vec{0} \\ \vec{0} \\ \vec{0} \end{pmatrix} - wg_2 c M^{-1} \begin{pmatrix} \vec{0} \\ \vec{1} \\ \vec{0} \\ \vec{0} \end{pmatrix} - wg_3 c M^{-1} \begin{pmatrix} \vec{0} \\ \vec{0} \\ \vec{1} \\ \vec{0} \end{pmatrix} - wg_4 c M^{-1} \begin{pmatrix} \vec{0} \\ \vec{0} \\ \vec{0} \\ \vec{1} \end{pmatrix} \quad (65)$$

where $c = \frac{1}{4} \frac{r_{\text{exo}}}{1 + H_{\text{IWG}} r_{\text{exo}}}$, $\vec{E} \in \mathbb{R}_{\geq 0}^{16}$, $\vec{1} = (1, 1, 1, 1)'$, and $\vec{0} = (0, 0, 0, 0)'$. Defining

$$L = \begin{pmatrix} 1 & 0 & 1 & 0 & 0 & 0 & 0 & 1 & 0 & 0 & 0 & 0 & 0 & 1 & 0 & 0 \\ 0 & 1 & 0 & 0 & 1 & 0 & 1 & 0 & 0 & 0 & 0 & 1 & 0 & 0 & 0 & 0 \\ 0 & 0 & 0 & 0 & 0 & 1 & 0 & 0 & 1 & 0 & 1 & 0 & 0 & 0 & 0 & 1 \\ 0 & 0 & 0 & 1 & 0 & 0 & 0 & 0 & 0 & 1 & 0 & 0 & 1 & 0 & 1 & 0 \end{pmatrix}$$

one obtains:

$$
\begin{pmatrix} \mathrm{EWG}_{\underline{1}} \\ \mathrm{EWG}_{\underline{2}} \\ \mathrm{EWG}_{\underline{3}} \\ \mathrm{EWG}_{\underline{4}} \end{pmatrix} = L\vec{E}.
$$

Theorem 1 (proved below) is equivalent to saying that:

$$
X = -cLM^{-1} \begin{pmatrix} \vec{0} \\ \vec{1} \\ \vec{0} \\ \vec{0} \end{pmatrix} = \begin{pmatrix} \beta_{\mathrm{med}} \\ \beta_{\mathrm{max}} \\ \beta_{\mathrm{med}} \\ \beta_{\mathrm{min}} \end{pmatrix}
$$

where: $\beta_{\mathrm{max}} > \beta_{\mathrm{med}} > \beta_{\mathrm{min}} > 0$. In fact, $X = (\mathrm{EWG}_1, \ldots, \mathrm{EWG}_4)$ corresponds to the solution of (56) when $wg = (0, 1, 0, 0)$, in which case $\mathrm{EWG}_{\underline{2}} = \beta_{\mathrm{max}}$, $\mathrm{EWG}_{\underline{1}} = \mathrm{EWG}_{\underline{3}} = \beta_{\mathrm{med}}$, and $\mathrm{EWG}_{\underline{4}} = \beta_{\mathrm{min}}$.

By symmetry of the system, it is easy to see that

$$
-cLM^{-1} \begin{pmatrix} \vec{1} \\ \vec{0} \\ \vec{0} \\ \vec{0} \end{pmatrix} = \begin{pmatrix} \beta_{\mathrm{max}} \\ \beta_{\mathrm{med}} \\ \beta_{\mathrm{min}} \\ \beta_{\mathrm{med}} \end{pmatrix}
$$

and so on (by circulating the positions of the β_*). Linear combination gives the general solution for the EWG_i.

Similarly, to compute the solution of (55), define

$$
Q = \begin{pmatrix} 1 & 1 & 1 & 1 & 0 & 0 & 0 & 0 & 0 & 0 & 0 & 0 & 0 & 0 & 0 & 0 \\ 0 & 0 & 0 & 0 & 1 & 1 & 1 & 0 & 0 & 0 & 0 & 0 & 0 & 0 & 0 & 0 \\ 0 & 0 & 0 & 0 & 0 & 0 & 0 & 0 & 1 & 1 & 1 & 1 & 0 & 0 & 0 & 0 \\ 0 & 0 & 0 & 0 & 0 & 0 & 0 & 0 & 0 & 0 & 0 & 0 & 1 & 1 & 1 & 1 \end{pmatrix}
$$

and recall that

$$
\begin{pmatrix} \mathrm{EWG}_{1,T} \\ \mathrm{EWG}_{2,T} \\ \mathrm{EWG}_{3,T} \\ \mathrm{EWG}_{4,T} \end{pmatrix} = Q\vec{E}.
$$

Now consider the solution for the case $wg = (0, 1, 0, 0)$:

$$Y = -cQM^{-1} \begin{pmatrix} \vec{0} \\ \vec{1} \\ \vec{0} \\ \vec{0} \end{pmatrix}$$

Using Facts E.1 and E.2, and then E.4 and E.6 (below), we define constants $\hat{\gamma}_{max} > \hat{\gamma}_{med} > \hat{\gamma}_{min} > 0$:

$$
\begin{aligned}
Y_1 &= 2E_{1,1} + E_{1,2} + E_{1,4} := \hat{\gamma}_{med}, \\
Y_2 &= 2E_{2,1} + 2E_{2,2} := \hat{\gamma}_{max}, \\
Y_3 &= 2E_{1,1} + E_{1,2} + E_{1,4} := \hat{\gamma}_{med}, \\
Y_4 &= 2E_{4,1} + 2E_{4,2} := \hat{\gamma}_{min},
\end{aligned}
$$

Substituion into (55) yields:

$$
\begin{pmatrix} Z_1 \\ Z_2 \\ Z_3 \\ Z_4 \end{pmatrix} = \frac{H_{IWG} r_{endo}}{1 + H_{IWG} r_{exo}} \begin{pmatrix} Y_1 \\ Y_2 \\ Y_3 \\ Y_4 \end{pmatrix} + \frac{1}{1 + H_{IWG} r_{exo}} \begin{pmatrix} 0 \\ 1 \\ 0 \\ 0 \end{pmatrix} = \begin{pmatrix} \hat{c}\hat{\gamma}_{med} \\ \tilde{c} + \hat{c}\hat{\gamma}_{max} \\ \hat{c}\hat{\gamma}_{med} \\ \hat{c}\hat{\gamma}_{min} \end{pmatrix}
$$

where $\hat{c} = \frac{H_{IWG} r_{endo}}{1 + H_{IWG} r_{exo}}$ and $\tilde{c} = \frac{1}{1 + H_{IWG} r_{exo}}$. Define:

$$\gamma_{max} = \tilde{c} + \hat{c}\hat{\gamma}_{max}, \quad \gamma_{med} = \hat{c}\hat{\gamma}_{med}, \quad \gamma_{min} = \hat{c}\hat{\gamma}_{min}.$$

The solutions for the cases $wg = (1, 0, 0, 0)$, $wg = (0, 0, 1, 0)$, $wg = (0, 0, 0, 1)$ are analogous (circulating the positions of the γ_*). An appropriate linear combination yields the desired result for IWG. □

Proof of Theorem 1 First, we state Facts E.1 and E.2, which hold for any wg.

Fact E.1 For all $i = 1, 2, 3, 4$ it holds that

$$EWG_{i,1} = EWG_{i,3}.$$

Proof This is easy to see from the respective equations:

$$
\begin{aligned}
&(-d + h)EWG_{i,1} + (r_M + h)EWG_{i,2} + (r_M + h)EWG_{i,3} + (r_M + h)EWG_{i,4} \\
&= -\frac{h}{r_{endo} H_{IWG}} wg_i \\
&(r_M + h)EWG_{i,1} + (r_M + h)EWG_{i,2} + (-d + h)EWG_{i,3} + (r_M + h)EWG_{i,4} \\
&= -\frac{h}{r_{endo} H_{IWG}} wg_i
\end{aligned}
$$

which can be rearranged to

$$
\begin{aligned}
-(d + r_M)\mathrm{EWG}_{i,1} + (r_M + h)(\mathrm{EWG}_{i,2} + \mathrm{EWG}_{i,4}) + (r_M + h) \\
\times (\mathrm{EWG}_{i,3} + \mathrm{EWG}_{i,1}) = -\frac{h}{r_{\mathrm{endo}} H_{\mathrm{IWG}}} wg_i \\
-(d + r_M)\mathrm{EWG}_{i,3} + (r_M + h)(\mathrm{EWG}_{i,2} + \mathrm{EWG}_{i,4}) + (r_M + h) \\
\times (\mathrm{EWG}_{i,3} + \mathrm{EWG}_{i,1}) = -\frac{h}{r_{\mathrm{endo}} H_{\mathrm{IWG}}} wg_i \ .
\end{aligned}
\tag{66}
$$

Subtracting these two equations yields the desired result. □

Fact E.2 It holds that

$$
\mathrm{EWG}_{2,2} = \mathrm{EWG}_{2,4}, \ \ \mathrm{EWG}_{4,2} = \mathrm{EWG}_{4,4}, \ \ \mathrm{EWG}_{1,2} = \mathrm{EWG}_{3,4}, \ \ \mathrm{EWG}_{1,4} = \mathrm{EWG}_{3,2}.
$$

Proof Exchanging the indexes:

$$
2, 2 \leftrightarrow 2, 4 \quad 4, 2 \leftrightarrow 4, 4 \quad 1, 2 \leftrightarrow 3, 4 \quad 1, 4 \leftrightarrow 3, 2
$$

it is easy to see that the system remains unchanged (see also Fig. 6). □

Assume now that $wg = (0, w, 0, 0)$, for any $w > 0$. The equality part in (13) is now clear:

Fact E.3 $\mathrm{EWG}_{\underline{1}} = \mathrm{EWG}_{\underline{3}}$.

Proof We first show that $\mathrm{EWG}_{1,1} = \mathrm{EWG}_{3,3}$. Writing Eq. (66) for $i = 1$ and $i = 3$:

$$
\begin{aligned}
-(d + r_M)\mathrm{EWG}_{1,1} + (r_M + h)(\mathrm{EWG}_{1,2} + \mathrm{EWG}_{1,4}) \\
+ (r_M + h)(\mathrm{EWG}_{1,3} + \mathrm{EWG}_{1,1}) = 0 \\
-(d + r_M)\mathrm{EWG}_{3,3} + (r_M + h)(\mathrm{EWG}_{3,2} + \mathrm{EWG}_{3,4}) \\
+ (r_M + h)(\mathrm{EWG}_{3,3} + \mathrm{EWG}_{3,1}) = 0
\end{aligned}
$$

Using Fact E.1 one has $\mathrm{EWG}_{1,1} = \mathrm{EWG}_{1,3}$ and $\mathrm{EWG}_{3,1} = \mathrm{EWG}_{3,3}$, and then using Fact E.2 obtains:

$$
\begin{aligned}
-(d + r_M - 2r_M - 2h)\mathrm{EWG}_{1,1} + (r_M + h)(\mathrm{EWG}_{3,4} + \mathrm{EWG}_{3,2}) = 0 \\
-(d + r_M - 2r_M - 2h)\mathrm{EWG}_{3,3} + (r_M + h)(\mathrm{EWG}_{3,2} + \mathrm{EWG}_{3,4}) = 0.
\end{aligned}
$$

Subtracting these two equations shows that $\mathrm{EWG}_{1,1} = \mathrm{EWG}_{3,3}$. Now recalling the notation for $X_{\underline{i}}$ from Appendix A

$$
\begin{aligned}
\mathrm{EWG}_{\underline{1}} = \mathrm{EWG}_{1,1} + \mathrm{EWG}_{2,4} + \mathrm{EWG}_{1,3} + \mathrm{EWG}_{4,2} \\
\mathrm{EWG}_{\underline{3}} = \mathrm{EWG}_{3,1} + \mathrm{EWG}_{4,4} + \mathrm{EWG}_{3,3} + \mathrm{EWG}_{2,2}.
\end{aligned}
$$

Using $EWG_{1,1} = EWG_{3,3}$, Facts E.1 and E.2 obtains:

$$EWG_1 = EWG_{3,1} + EWG_{2,2} + EWG_{3,3} + EWG_{4,4} = EWG_3.$$

as we wanted to prove. □

To show the other inequalities, note first that the 16 variables $EWG_{i,j}$ are thus reduced to only seven:

$$
\begin{aligned}
E_{1,1} &= EWG_{1,1} = EWG_{1,3} = EWG_{3,1} = EWG_{3,3} \\
E_{1,2} &= EWG_{1,2} = EWG_{3,4} \\
E_{1,4} &= EWG_{1,4} = EWG_{3,2} \\
E_{2,1} &= EWG_{2,1} = EWG_{2,3} \\
E_{2,2} &= EWG_{2,2} = EWG_{2,4} \\
E_{4,1} &= EWG_{4,1} = EWG_{4,3} \\
E_{4,2} &= EWG_{4,2} = EWG_{4,4}
\end{aligned}
$$

and satisfy the equations:

$$- (d - r_M - 2h)E_{1,1} + (r_{LM} + h)E_{1,2} + (r_{LM} + h)E_{1,4} = 0 \tag{67}$$

$$2(r_{LM} + h)E_{1,1} - (d - h)E_{1,2} + hE_{1,4} + r_M E_{2,2} = 0 \tag{68}$$

$$2(r_{LM} + h)E_{1,1} + hE_{1,2} - (d - h)E_{1,4} + r_M E_{4,2} = 0 \tag{69}$$

$$-(d - r_M - 2h)E_{2,1} + 2(r_{LM} + h)E_{2,2} = -\frac{h}{r_{endo} H_{IWG}} wg_2 \tag{70}$$

$$2(r_{LM} + h)E_{2,1} - (d - 2h)E_{2,2} + r_M E_{1,2} = -\frac{h}{r_{endo} H_{IWG}} wg_2 \tag{71}$$

$$-(d - r_M - 2h)E_{4,1} + 2(r_{LM} + h)E_{4,2} = 0 \tag{72}$$

$$2(r_{LM} + h)E_{4,1} - (d - 2h)E_{4,2} + r_M E_{1,4} = 0 . \tag{73}$$

To simplify notation, set:

$$A = d - r_M - 2h, \quad B = 2(r_{LM} + h), \quad \bar{w} = \frac{h}{r_{endo} H_{IWG}} wg_2,$$

and note that $A > B > 0$.

Fact E.4 The following hold:

(a) $E_{4,1} < E_{4,2} < E_{1,4} < E_{1,2} < E_{2,2}$;
(b) $E_{4,1} < E_{1,1} < E_{1,2}$;
(c) $E_{1,2} + E_{1,4} < E_{2,2} + E_{4,2}$

Proof To prove part (a), from Eqs. (72) and (73) it holds that

$$E_{4,1} = \frac{B}{A} E_{4,2}; \quad E_{4,2} = \frac{r_M A}{A^2 - B^2 + r_M A} E_{1,4}$$

Because $A > B > 0$, it is clear that $E_{4,1} < E_{4,2} < E_{1,4}$. From Eqs. (70) and (71) it holds that

$$E_{2,1} = \frac{B}{A} E_{2,2} + \frac{1}{A} \bar{w}; \quad E_{2,2} = \frac{r_M A}{A^2 - B^2 + r_M A} E_{1,2} + \frac{A + B}{A^2 - B^2 + r_M A} \bar{w}$$

Then Eqs. (68) and (69) can be written in the form

$$\left(d - r_M \frac{r_M A}{A^2 - B^2 + r_M A} \right) E_{1,2} = B E_{1,1} + h(E_{1,2} + E_{1,4}) + r_M \frac{A + B}{A^2 - B^2 + r_M A} \bar{w}$$

$$\left(d - r_M \frac{r_M A}{A^2 - B^2 + r_M A} \right) E_{1,4} = B E_{1,1} + h(E_{1,2} + E_{1,4})$$

which implies that $E_{1,4} < E_{1,2}$ (it is easy to see that the factor multiplying both $E_{1,2}$ and $E_{1,4}$ is positive, since $d > r_M$).

We still need to prove the last inequality in (a), but we can now prove (b). From Eq. (67)

$$E_{1,1} = \frac{1}{2} \frac{B}{A} (E_{1,2} + E_{1,4}) < E_{1,2}$$

using (a) and because $B < A$. This proves the second inequality in (b). To prove (c), substitute this $E_{1,1}$ expression into the sum of Eqs. (68) and (69):

$$E_{2,2} + E_{4,2} = \frac{A^2 - B^2 + r_M A}{r_M A} (E_{1,2} + E_{1,4}) > E_{1,2} + E_{1,4}.$$

The last part of (a) now follows from (c) together with $E_{4,2} < E_{1,4}$, which implies $E_{1,2} < E_{2,2}$.

Finally, the first part of (b) is easy to see from:

$$E_{1,1} - E_{4,1} = \frac{1}{2} \frac{B}{A} (E_{1,2} + E_{1,4}) - \frac{B}{A} E_{4,2} > \frac{1}{2} \frac{B}{A} (E_{1,2} + E_{1,4} - E_{1,4}) > 0.$$

$\square$

To prove the first inequality of Theorem 1 is now straighforward.

Fact E.5 $EWG_4 < EWG_1$

Proof Recall the notation for EWG_i and use Fact E.4

$$EWG_1 - EWG_4 = 2E_{1,1} + E_{2,2} + E_{4,2} - 2E_{4,1} - 2E_{1,4}$$

$$= 2(E_{1,1} - E_{4,1}) + (E_{2,2} + E_{4,2} - E_{1,2} - E_{1,4}) + (E_{1,2} - E_{1,4}) > 0.$$

$\square$

To prove the other inequality we need the next result.

Fact E.6 It holds that: $E_{2,1} > E_{2,2}$.

Proof First notice that

$$E_{1,2} = r_M \frac{A + B}{d(A^2 - B^2 + r_M A) - r_M^2 A} \bar{w}$$
$$+ \frac{1}{2} r_M \frac{A^2 - B^2 + r_M A}{d(A^2 - B^2 + r_M A) - r_M^2 A} \frac{-A^2 + B^2 + (d - r_M)A}{(A - B)(A^2 - B^2 + 2r_M A)} \bar{w}.$$

Now consider

$$E_{2,1} - E_{2,2} = -\frac{A - B}{A} \frac{r_M A}{A^2 - B^2 + r_M A} E_{1,2} - \frac{A - B}{A} \frac{A + B}{A^2 - B^2 + r_M A} \bar{w} + \frac{1}{A} \bar{w}.$$

The last two terms can be combined into

$$\frac{r_M}{A^2 - B^2 + r_M A} \bar{w},$$

and the two terms due to $E_{1,2}$ can be simplified to:

$$-r_M \frac{1}{A^2 - B^2 + r_M A} \frac{(A - B)(A + B)}{\frac{d}{r_M}(A^2 - B^2 + r_M A) - r_M A} \bar{w}$$

and

$$-\frac{r_M}{2} \frac{1}{A^2 - B^2 + 2r_M A} \frac{-A^2 + B^2 + (d - r_M)A}{\frac{d}{r_M}(A^2 - B^2 + r_M A) - r_M A} \bar{w}.$$

Factoring out $r_M \bar{w} / \left(\frac{d}{r_M}(A^2 - B^2 + r_M A) - r_M A \right)$, one obtains

$$\frac{1}{r_M \bar{w}} \left(\frac{d}{r_M}(A^2 - B^2 + r_M A) - r_M A \right) (E_{2,1} - E_{2,2})$$

$$= \frac{1}{A^2 - B^2 + r_M A} \left(\frac{d}{r_M}(A^2 - B^2 + r_M A) - r_M A - (A^2 - B^2) \right)$$

$$- \frac{1}{2} \frac{-A^2 + B^2 + (d - r_M)A}{A^2 - B^2 + 2r_M A}$$

which can be further simplified to

$$\frac{\left(\frac{d}{r_M} - 1 \right)(A^2 - B^2)}{A^2 - B^2 + r_M A} + \frac{1}{2} \frac{A^2 - B^2}{A^2 - B^2 + 2r_M A}$$

$$+ \frac{(d - r_M)A}{A^2 - B^2 + r_M A} - \frac{1}{2} \frac{(d - r_M)A}{A^2 - B^2 + 2r_M A} > 0$$

because the first two terms are clearly positive, and the last two terms add up to a positive number. This shows that $E_{2,1} > E_{2,2}$, as we wanted to prove. □

The proof of Theorem 1 can now be completed.

Fact E.7 $EWG_1 < EWG_2$.

Proof Consider:

$$EWG_2 - EWG_1 = 2E_{2,1} + 2E_{1,2} - 2E_{1,1} - E_{2,2} - E_{4,2}$$
$$= 2(E_{1,2} - E_{1,1}) + (E_{2,1} - E_{2,2}) + (E_{2,1} - E_{4,2}),$$

which is positive because $E_{1,2} > E_{1,1}$ [Lemma E.4(b)], and $E_{2,1} > E_{2,2} > E_{4,2}$ (Lemmas E.4(a) and E.6). □

Appendix F: Analytically solving PTC and HH levels

In this section, we prove uniqueness of solutions for PTC and HH given any set of parameters $p_{\text{PTC-HH}}$ (see (16)), and $hh = (0, 1, 0, 0)$ and $ptc = (T_1, T_2, 0, T_4)$, with $T_2 = T_4$. The steady state levels of Patched and Hedgehog proteins are given by a system of nonlinear Eqs. (58) and (63). These equations can be solved explicitly and uniquely in the case $ptc_2 = ptc_4 = T_2$, which is true if the steady state is in $\mathcal{W}$. To simplify notation, we use

$$r_P = r_{LM\text{PTC}}, \quad r_H = r_{LM\text{HH}}, \quad \kappa_H = \kappa_{\text{PTCHH}}[\text{HH}]_0, \quad \kappa_P = \kappa_{\text{PTCHH}}[\text{PTC}]_0,$$

and define

$$d_P = \frac{1}{H_{\text{PTC}}} + 2r_P, \quad d_H = \frac{1}{H_{\text{HH}}} + 2r_H.$$

We introduce further notation:

$$\beta_P = \frac{2r_P^2 d_P}{d_P^2 - 2r_P^2}, \quad \gamma_P = \frac{1}{4H_{\text{PTC}}} + \frac{1}{4H_{\text{PTC}}}\frac{2r_P(r_P + d_P)}{d_P^2 - 2r_P^2} = \frac{1}{4H_{\text{PTC}}}\frac{d_P(2r_P + d_P)}{d_P^2 - 2r_P^2}.$$

Lemma F.1 *Let* $x \in \mathcal{W}$. *Then, the solution for HH is:*

$$HH_{i,1} = HH_{i,2} = HH_{i,3} = HH_{i,4} = 0, \quad i = 1, 2, 4,$$
$$HH_{3,2} = HH_{3,4} = Root_+,$$
$$HH_{3,1} = HH_{3,3} = \frac{1}{d_H}\left(\frac{1}{4}\frac{hh_3}{H_{\text{HH}}} + r_H HH_{3,2} + r_H HH_{3,4}\right),$$

where Root$_+$ *is the positive root of the quadratic equation*:

$$k_H(d_H^2 - 4r_H^2)X^2 + \left((d_P - \beta_P)(d_H^2 - 4r_H^2) - k_H(d_H + 2r_H)\frac{hh_3}{4H_{HH}} + d_H k_P \gamma_P ptc_2\right)X$$
$$- (d_P - \beta_P)(d_H + 2r_H)\frac{hh_3}{4H_{HH}} = 0.$$

And the solution for PTC is:

$$PTC_{3,1} = PTC_{3,2} = PTC_{3,3} = PTC_{3,4} = 0,$$
$$PTC_{2,2} = PTC_{4,4} = \frac{\gamma_P T_2}{d_P - \beta_P + k_H HH_{3,4}},$$
$$PTC_{2,1} = PTC_{2,3} = PTC_{4,1} = PTC_{4,3}$$
$$= \frac{1}{d_P^2 - 2r_P^2}\left(r_P d_P PTC_{2,2} + \frac{1}{4H_{PTC}}(d_P + r_P)T_2\right),$$
$$PTC_{2,4} = PTC_{4,2} = \frac{1}{d_P}\left(\frac{1}{4}\frac{T_2}{H_{PTC}} + 2r_P PTC_{2,1}\right).$$

Proof Let $x \in \mathcal{W}$ and $h(x)$ be a vector defined by (3). Because *hedgehog* is not expressed in cells 1, 2 and 4, note that for $i = 1, 2, 4$

$$HH_{i,\text{T}} = \sum_{j=1}^{4} HH_{i,j} = hh_i - \kappa_P(\cdots) + r_H \sum_{j=1}^{4}(HH_{i,j+1} + HH_{i,j-1} - 2HH_{i,j})$$
$$= -\kappa_P(\cdots)$$

since $hh = (0, 0, 1, 0)$, and the sum that multiplies r_H cancels out. The terms in $\kappa_P(\cdots)$ are all nonnegative, and therefore they can only be zero. We conclude that:

$$HH_{i,1} = HH_{i,2} = HH_{i,3} = HH_{i,4} = 0, \quad i = 1, 2, 4.$$

A similar argument shows that $ptc_3 = 0$ implies:

$$PTC_{3,1} = PTC_{3,2} = PTC_{3,3} = PTC_{3,4} = 0.$$

Therefore, the only nonlinear terms appear in the equations for PTC$_{2,2}$ and PTC$_{4,4}$:

$$d_P PTC_{2,2} - r_P PTC_{2,1} - r_P PTC_{2,3} + \kappa_H PTC_{2,2} HH_{3,4} = \frac{1}{4H_{PTC}}ptc_2$$
$$d_P PTC_{4,4} - r_P PTC_{4,1} - r_P PTC_{4,3} + \kappa_H PTC_{4,4} HH_{3,2} = \frac{1}{4H_{PTC}}ptc_4.$$

Moreover, symmetry of the system shows that $PTC_{2,1} = PTC_{2,3}$ and $PTC_{4,1} = PTC_{4,3}$, because each pair satisfies exactly the same equation:

$$d_P PTC_{2,1} - r_P PTC_{2,2} - r_P PTC_{2,4} = \frac{1}{4H_{\text{PTC}}} ptc_2 \qquad (74)$$

$$d_P PTC_{4,3} - r_P PTC_{4,4} - r_P PTC_{4,2} = \frac{1}{4H_{\text{PTC}}} ptc_4. \qquad (75)$$

We then have:

$$PTC_{2,4} = \frac{1}{d_P} \left(\frac{1}{4H_{\text{PTC}}} ptc_2 + 2r_P PTC_{2,1} \right)$$

$$PTC_{4,2} = \frac{1}{d_P} \left(\frac{1}{4H_{\text{PTC}}} ptc_4 + 2r_P PTC_{4,1} \right).$$

Solving for $PTC_{2,1}$ as a function of $PTC_{2,2}$, and for $PTC_{4,1}$ as a function of $PTC_{4,4}$:

$$PTC_{2,1} = \frac{1}{d_P^2 - 2r_P^2} \left(r_P d_P PTC_{2,2} + \frac{1}{4H_{\text{PTC}}} (d_P + r_P) ptc_2 \right)$$

$$PTC_{4,1} = \frac{1}{d_P^2 - 2r_P^2} \left(r_P d_P PTC_{4,4} + \frac{1}{4H_{\text{PTC}}} (d_P + r_P) ptc_4 \right).$$

Thus we get equations depending only on $PTC_{2,2}$ and $HH_{3,4}$, and on $PTC_{4,4}$ and $HH_{3,2}$:

$$d_P PTC_{2,2} - \frac{2r_P}{d_P^2 - 2r_P^2} \left(r_P d_P PTC_{2,2} + \frac{1}{4H_{\text{PTC}}} (d_P + r_P) ptc_2 \right)$$

$$+ \kappa_H PTC_{2,2} HH_{3,4} = \frac{1}{4H_{\text{PTC}}} ptc_2 \qquad (76)$$

$$d_P PTC_{4,4} - \frac{2r_P}{d_P^2 - 2r_P^2} \left(r_P d_P PTC_{4,4} + \frac{1}{4H_{\text{PTC}}} (d_P + r_P) ptc_4 \right)$$

$$+ \kappa_H PTC_{4,4} HH_{3,2} = \frac{1}{4H_{\text{PTC}}} ptc_4 . \qquad (77)$$

On the other hand, since $PTC_{3,j} = 0$ for all j, it follows that:

$$HH_{3,1} = HH_{3,3} = \frac{1}{d_H} \left(\frac{1}{4H_{\text{HH}}} hh_3 + r_H HH_{3,2} + r_H HH_{3,4} \right),$$

and substituting into the $HH_{3,4}$ and $HH_{3,2}$ equations:

$$d_H HH_{3,4} - 2\frac{r_H}{d_H}\left(\frac{1}{4H_{HH}}hh_3 + r_H HH_{3,2} + r_H HH_{3,4}\right)$$
$$- \kappa_P PTC_{2,2} HH_{3,4} = \frac{1}{4H_{HH}}hh_3 \qquad (78)$$

$$d_H HH_{3,2} - 2\frac{r_H}{d_H}\left(\frac{1}{4H_{HH}}hh_3 + r_H HH_{3,2} + r_H HH_{3,4}\right)$$
$$- \kappa_P PTC_{4,4} HH_{3,2} = \frac{1}{4H_{HH}}hh_3. \qquad (79)$$

The last four equations may be solved for the four variables $PTC_{2,2}$, $PTC_{4,4}$, $HH_{3,2}$ and $HH_{3,4}$, and the remaining PTC, HH will then follow. Recalling the notation introduced above, one can write

$$PTC_{2,2} = \frac{\gamma_P ptc_2}{d_P - \beta_P + k_H HH_{3,4}}, \quad PTC_{4,4} = \frac{\gamma_P ptc_4}{d_P - \beta_P + k_H HH_{3,2}}. \qquad (80)$$

This leads to

$$d_H HH_{3,4} - 2\frac{r_H}{d_H}\left(\frac{1}{4H_{HH}}hh_3 + r_H HH_{3,2} + r_H HH_{3,4}\right)$$
$$- \kappa_P \gamma_P ptc_2 \frac{HH_{3,4}}{d_P - \beta_P + k_H HH_{3,4}} = \frac{1}{4H_{HH}}hh_3$$

$$d_H HH_{3,2} - 2\frac{r_H}{d_H}\left(\frac{1}{4H_{HH}}hh_3 + r_H HH_{3,2} + r_H HH_{3,4}\right)$$
$$- \kappa_P \gamma_P ptc_4 \frac{HH_{3,2}}{d_P - \beta_P + k_H HH_{3,2}} = \frac{1}{4H_{HH}}hh_3 .$$

From the symmetry of these equations, it is easy to see that

$$ptc_2 = ptc_4 \quad \Rightarrow \quad HH_{3,4} = HH_{3,2}.$$

and thus have the following equation for $HH_{3,4} = HH_{3,2} = X$ (after some simple algebra steps):

$$k_H(d_H^2 - 4r_H^2)X^2 + \left((d_P - \beta_P)(d_H^2 - 4r_H^2) - k_H(d_H + 2r_H)\frac{hh_3}{4H_{HH}}\right.$$
$$\left.+ d_H k_P \gamma_P ptc_2\right) X - (d_P - \beta_P)(d_H + 2r_H)\frac{hh_3}{4H_{HH}} = 0. \qquad (81)$$

We next show that only one of the two roots of this second order polynomial is positive and hence the unique solution to $HH_{3,2}$, $HH_{3,4}$. Let the polynomial be of the form

$c_2 X^2 + c_1 X + c_0 = 0$. The term inside the square root will be $c_1^2 - 4c_0 c_2$ where:

$$-4c_0 c_2 = 4k_H (d_H^2 - 4r_H^2)(d_P - \beta_P)(d_H + 2r_H)\frac{hh_3}{4H_{\text{HH}}}.$$

The factor $d_H^2 - 4r_H^2$ is positive, by definition of d_H. The factor

$$d_P - \beta_P = d_P - \frac{2r_P^2 d_P}{d_P^2 - 2r_P^2} = d_P(d_P^2 - 4r_P^2)$$

is also positive, again by definition of d_P. This means that $c_1^2 - 4c_0 c_2 > c_1^2$, so whatever the sign of c_1, $-c_1 - \sqrt{c_1^2 - 4c_0 c_2} < 0$, which leaves us with:

$$\text{HH}_{3,2} = \text{HH}_{3,4} = \frac{-c_1 + \sqrt{c_1^2 - 4c_0 c_2}}{2c_2}$$

(the coefficients are as in (81)). $\qquad\square$

Appendix G: The regulation of cubitus proteins

The cubitus interruptus activator and repressor proteins may only be expressed whenever engrailed is absent. In addition, they auto-regulate themselves through patched mRNA and protein. Using $\text{EN} = en$ note that CI can be written in terms of CN:

$$\text{CI}_i = ci_i - \text{CN}_i = U_i \theta^-(en_i, \kappa_{\text{ENci}}) - \text{CN}_i$$

Note that, if $Y = U - X$:

$$\theta^+(X, \kappa_a) = \theta^-(Y, U - \kappa_a).$$

Furthermore,

$$\theta^-(Y, U - \kappa_a)\theta^-(Y, \kappa_b) = \theta^-(Y, \min\{U - \kappa_a, \kappa_b\}).$$

Then *ptc* can be simplified as follows:

$$\begin{aligned}
ptc_i &= \theta^+(\text{CI}_i \theta^-(\text{CN}_i, \kappa_{\text{CNptc}}), \kappa_{\text{CNptc}})) \\
&= \begin{cases} \theta^+(\text{CI}_i, \kappa_{\text{CIptc}})\theta^-(\text{CN}_i, \kappa_{\text{CNptc}}), & \text{CN}_i \neq \kappa_{\text{CNptc}} \\ \theta^+(\text{CI}_i, \kappa_{\text{CIptc}}), & \text{CN}_i = \kappa_{\text{CNptc}} \end{cases} \\
&= \begin{cases} \theta^-(\text{CN}_i, \min\{ci_i - \kappa_{\text{CIptc}}, \kappa_{\text{CNptc}}\}), & \text{CN}_i \neq \kappa_{\text{CNptc}} \\ \theta^-(\text{CN}_i, ci_i - \kappa_{\text{CIptc}}), & \text{CN}_i = \kappa_{\text{CNptc}} \end{cases}
\end{aligned} \qquad (82)$$

ptc is used to compute PTC explicitly (as in Sect. F), which feeds back into CN:

$$
\begin{aligned}
\mathrm{CN}_i &= ci_i \frac{H_{\mathrm{CI}} C_{\mathrm{CI}} \theta^+ (\mathrm{PTC}_{i,T}, \kappa_{\mathrm{PTCCI}})}{1 + H_{\mathrm{CI}} C_{\mathrm{CI}} \theta^+ (\mathrm{PTC}_{i,T}, \kappa_{\mathrm{PTCCI}})} \\
&= U_i \theta^- (en_i, \kappa_{\mathrm{EN}ci}) \frac{H_{\mathrm{CI}} C_{\mathrm{CI}} \theta^+ (\mathrm{PTC}_{i,T}, \kappa_{\mathrm{PTCCI}})}{1 + H_{\mathrm{CI}} C_{\mathrm{CI}} \theta^+ (\mathrm{PTC}_{i,T}, \kappa_{\mathrm{PTCCI}})}.
\end{aligned}
$$

Throughout this paper, we will consider that $\theta^-(en_3, \kappa_{\mathrm{EN}ci}) = 0$ and $\theta^-(en_i, \kappa_{\mathrm{EN}ci}) = 1$ for $i = 1, 2, 4$. In addition, defining $Q_i = 1$ if $\mathrm{PTC}_{i,T} > \kappa_{\mathrm{PTCCI}}$, $Q_i = 0$ if $\mathrm{PTC}_{i,T} < \kappa_{\mathrm{PTCCI}}$, and $Q_i \in [0, 1]$ if $\mathrm{PTC}_{i,T} = \kappa_{\mathrm{PTCCI}}$, we have:

$$
\mathrm{CN}_i = U_i \frac{Q_i H_{\mathrm{CI}} C_{\mathrm{CI}}}{1 + Q_i H_{\mathrm{CI}} C_{\mathrm{CI}}}. \tag{83}
$$

Appendix H: Computing the cylindrical algebraic decomposition

A CAD for the parameter space G can be computed from Eqs. (52)–(63), by imposing the conditions $x \in \mathcal{W}$, as given by (7). Following von Dassow et al.'s criteria, conditions on wild type expression of *en*, *hh*, and *wg* at steady state, are obtained from a threshold expression:

$$
en_3^{\mathrm{WT}} \geq \varepsilon \quad \text{and} \quad en_i^{\mathrm{WT}} < \varepsilon, \quad i = 1, 2, 4 \tag{84}
$$

$$
hh_3^{\mathrm{WT}} \geq \varepsilon \quad \text{and} \quad hh_i^{\mathrm{WT}} < \varepsilon, \quad i = 1, 2, 4 \tag{85}
$$

$$
wg_2^{\mathrm{WT}} \geq \varepsilon \quad \text{and} \quad wg_i^{\mathrm{WT}} < \varepsilon, \quad i = 1, 3, 4. \tag{86}
$$

Throughout this paper, we will consider also that

$$
ci_3^{\mathrm{WT}} < \varepsilon \quad \text{and} \quad ci_i^{\mathrm{WT}} \geq \varepsilon, \quad i = 1, 2, 4, \tag{87}
$$

$$
ptc_3^{\mathrm{WT}} < \varepsilon \quad \text{and} \quad ptc_i^{\mathrm{WT}} \geq \varepsilon, \quad i = 1, 2, 4, \tag{88}
$$

thus incorporating further experimental data [18,19] into the analysis.

We will make four assumptions, only slightly stronger then (85), (87)–(89), but which allow to obtain clean analytical results for a large part of the problem of finding the feasible parameter space. These analytical results include Theorem 1 (for establishing symmetry of EWG) and explicit computation of PTC and HH. The modified assumptions are:

$$
en_3^{\mathrm{WT}} \geq \varepsilon \quad \text{and} \quad en_i^{\mathrm{WT}} = 0, \quad i = 1, 2, 4 \tag{89}
$$

$$
wg_2^{\mathrm{WT}} \geq \varepsilon \quad \text{and} \quad wg_4 \leq \min_{i=1,3} wg_i^{\mathrm{WT}} < \varepsilon \tag{90}
$$

$$
ci_3^{\mathrm{WT}} = 0 \quad \text{and} \quad ci_i^{\mathrm{WT}} \geq \varepsilon, \quad i = 1, 2, 4 \tag{91}
$$

$$
ptc_3^{\mathrm{WT}} < \varepsilon \quad \text{and} \quad ptc_2^{\mathrm{WT}} = ptc_4^{\mathrm{WT}}, ptc_1^{\mathrm{WT}} \geq \varepsilon, \tag{92}
$$

Then, from (82) and (91), it is clear that:

$$CI_3 = CN_3 \equiv 0 \quad \text{and} \quad ptc_3 \equiv 0.$$

H.1 p_{CI}, p_{PTC-HH}, p_{WG}, α_{CIwg}

As already remarked, a CAD is not unique, and the choice of the "free" parameters, or those that come at the top of the hierarchy have to be chosen. In this case, we choose the parameters and intervals already listed in (16), which form S_1. von Dassow et al. chose the interval [5, 100] for half-lives (H_X) and (0, 1] for ON/OFF parameters (κ_{XY}) to denote the range of *physiological* values. This is reasonable since, by model construction, all variables are "normalized" to 1. Assuming ON/OFF constants $\kappa_{XY} > 1$ would amount to assume that Y is permanently activated (or inhibited) by X.

Lemma H.1 *Assume conditions* (85), (89), *and* (91) *hold. Then* κ_{ENci}, $\kappa_{ENhh} \in (0, \sigma_{en3}]$, $\kappa_{CNhh} \in (0, 1]$. *Also* $U_3 \in [0, 1]$, $U_{1,2,4} \in [\varepsilon, 1]$.

Proof Recalling (59) and EN $= en$, conditions (91) can be re-written:

$$en_3 > \kappa_{ENci} \quad \text{and} \quad en_{1,2,4} \leq \kappa_{ENci}.$$

These are equivalent to $\kappa_{ENci} \in [\max\{en_i, i = 1, 2, 4\}, en_3)$. From (89), $\max\{en_i, i = 1, 2, 4\} = 0$ and $en_3 = \sigma_{en3} \in [\varepsilon, 1]$ denotes the possible values of $\theta^-(EWG_3, \kappa_{WGwg})$ when $EWG_3 = \kappa_{WGwg}$. Next, since $ci_3 = 0$ due to $\theta^-(EN_3, \kappa_{ENci}) = 0$, U_3 can take any value in [0, 1], and $U_{1,2,4}$ have to be larger than the thresdold ε.

Conditions (85) translate to:

$$en_3 \geq \kappa_{ENhh} \quad \text{and} \quad CN_3 \leq \kappa_{CNhh}$$
$$en_i \leq \kappa_{ENhh} \quad \text{or} \quad CN_i \geq \kappa_{CNhh}, \quad i = 1, 2, 4. \tag{93}$$

Since $en_{1,2,4} = 0$, no restrictions on κ_{CNhh} are needed, so $\kappa_{CNhh} \in (0, 1]$. Since $CN_3 = 0$, all conditions are verified iff $\kappa_{ENhh} \in (0, \sigma_{en3}]$. □

H.2 κ_{PTCCI}, κ_{CIptc}, and κ_{CNptc}

For simplicity, here we will treat the case $wg_2 > 0$, $wg_i = 0$ ($i = 1, 3, 4$). As shown below (Sect. H.3), this is true for almost all feasible sets of parameters. It also implies that $EWG_1 = EWG_3$.

Lemma H.2 *For system* (1) *with steady state set* (7), *the following hold:*

(a) $\kappa_{PTCCI} \in (0, \min\{T_1, PTC_{2,T}^{WT}\}]$;

(b) $\kappa_{CNptc} \in \left[\max_{i=1,2,4} U_i \frac{Q_i H_{CI} C_{CI}}{1+Q_i H_{CI} C_{CI}}, 1\right]$;

(c) $\kappa_{CIptc} \in \left(0, \min_{i=1,2,4} \frac{U_i}{1+Q_i H_{CI} C_{CI}}\right]$.

Proof By assumption (92) (and definition of $\mathcal{W}$), $ptc_2^{\text{WT}} = ptc_4^{\text{WT}}$, By Lemma F.1 in Appendix F, we then have $\text{PTC}_{2,T} = \text{PTC}_{4,T}$. By Theorem 1 and (89) it follows that $\text{CN}_2^{\text{WT}} > 0$ is always required for a nonemtpy parameter set. In the case EWG_1EWG_3, Theorem 1 also shows that $\text{CN}_1^{\text{WT}} > 0$ is necessary. From Appendix G this can only be achieved iff $\kappa_{\text{PTCCI}} \leq \{\text{PTC}_{1,T}, \text{PTC}_{2,T}\}$ where $\text{PTC}_{1,T} = T_1$. We can write, for $i = 1, 2, 4$:

$$ptc_i = \begin{cases} \theta^-(\text{CN}_i, \min\{U_i - \kappa_{\text{CIptc}}, \kappa_{\text{CNptc}}\}), & \text{CN}_i \neq \kappa_{\text{CNptc}} \\ \theta^-(\text{CN}_i, U_i - \kappa_{\text{CIptc}}), & \text{CN}_i = \kappa_{\text{CNptc}} \end{cases}$$

and (from $\mathcal{W}$) $ptc_i \geq \varepsilon$, for $i = 1, 2, 4$. This implies $\text{CN}_i \leq \min\{U_i - \kappa_{\text{CIptc}}, \kappa_{\text{CNptc}}\}$ which translates into intervals (b) and (c). □

H.3 κ_{WGen}, κ_{CNen}, κ_{WGwg}, κ_{CNwg}, and κ_{CIwg}

Recall the expression of wg at steady state, given in (12). For most sets of parameters, it will happen that $R_{\text{CI}}, R_{\text{WG}} \in \{0, 1\}$, yielding four possible values for wg_i:

$$wg_i \in \left\{0, \frac{\alpha_{\text{WG}}}{1 + \alpha_{\text{WG}}}, \frac{\alpha_{\text{CI}}}{1 + \alpha_{\text{CI}}}, \frac{\alpha_{\text{CI}} + \alpha_{\text{WG}}}{1 + \alpha_{\text{CI}} + \alpha_{\text{WG}}}\right\}.$$

For the cases when variables CI, CN or IWG fall on their threshold values, $\text{CI}_i = \kappa_{\text{CIwg}}$, $\text{CN}_i = \kappa_{\text{CNwg}}$ and/or $\text{IWG}_i = \kappa_{\text{WGwg}}$, it will happen that $R_{\text{CI}}, R_{\text{WG}} \in [0, 1]$. Since these cases imply a fine tuning of κ_{CIwg}, κ_{CNwg}, or κ_{WGwg}, they will happen for a much smaller family of parameters. Therefore, in this Section, we analyze only the case $R_{\text{CI}}, R_{\text{WG}} \in \{0, 1\}$. (However, note that the product "$R_{\text{CI}}\alpha_{\text{CI}}$" can be treated as a new "α_{CI}", and hence the cases $R_{\text{CI,WG}} \in (0, 1)$ may be analyzed in a similar way.)

According to the choice of α_{CI} and α_{WG} in (16), we have:

$$\varepsilon \leq \min\left\{\frac{\alpha_{\text{WG}}}{1 + \alpha_{\text{WG}}}, \frac{\alpha_{\text{CI}}}{1 + \alpha_{\text{CI}}}\right\}$$

In this case, either the cubitus pathway or the wingless pathway may maintain *wingless* in the second cell, and both pathways need to be shutdown on the other cells:

$$wg_2 \in \left\{\frac{\alpha_{\text{WG}}}{1 + \alpha_{\text{WG}}}, \frac{\alpha_{\text{CI}}}{1 + \alpha_{\text{CI}}}, \frac{\alpha_{\text{CI}} + \alpha_{\text{WG}}}{1 + \alpha_{\text{CI}} + \alpha_{\text{WG}}}\right\} \quad \text{and} \quad wg_i = 0, \quad i = 1, 3, 4,$$

Conditions (89) can then be written as inequalities on wg and CN:

$$\text{EWG}_3 = wg_2\beta_{\text{med}} \geq \kappa_{\text{WGen}} \quad \text{and} \quad \text{CN}_3 \leq \kappa_{\text{CNen}}, \tag{94a}$$

$$\text{EWG}_1 = wg_2\beta_{\text{med}} < \kappa_{\text{WGen}} \quad \text{or} \quad \text{CN}_1 > \kappa_{\text{CNen}}, \tag{94b}$$

$$\text{EWG}_2 = wg_2\beta_{\text{max}} < \kappa_{\text{WGen}} \quad \text{or} \quad \text{CN}_2 > \kappa_{\text{CNen}}, \tag{94c}$$

$$\text{EWG}_4 = wg_2\beta_{\text{min}} < \kappa_{\text{WGen}} \quad \text{or} \quad \text{CN}_4 > \kappa_{\text{CNen}}. \tag{94d}$$

Since $\beta_{\max} > \beta_{\mathrm{med}}$, it is clear that (94a–c) can only be satisfied if

$$\mathrm{CN}_1, \mathrm{CN}_2 > \kappa_{\mathrm{CN}en}.$$

Conditions (90) translate to:

$$
\begin{aligned}
wg_2\gamma_{\max} &\geq \kappa_{\mathrm{WG}wg} \quad \text{or} \quad \mathrm{CN}_2 \leq \min\{\kappa_{\mathrm{CN}wg}, U_2 - \kappa_{\mathrm{CI}wg}\}, \\
wg_2\gamma_{\mathrm{med}} &\leq \kappa_{\mathrm{WG}wg} \quad \text{and} \quad \mathrm{CN}_1 \geq \min\{\kappa_{\mathrm{CN}wg}, U_1 - \kappa_{\mathrm{CI}wg}\}, \\
wg_2\gamma_{\mathrm{med}} &\leq \kappa_{\mathrm{WG}wg} \quad \text{and} \quad \mathrm{CN}_3 \geq \min\{\kappa_{\mathrm{CN}wg}, 0 - \kappa_{\mathrm{CI}wg}\}, \\
wg_2\gamma_{\min} &\leq \kappa_{\mathrm{WG}wg} \quad \text{and} \quad \mathrm{CN}_4 \geq \min\{\kappa_{\mathrm{CN}wg}, U_4 - \kappa_{\mathrm{CI}wg}\}.
\end{aligned}
\tag{95}
$$

From (91) it follows that $\mathrm{CN}_3 = 0$. So the inequalities that represent en^{WT} and wg^{WT}

Table 3 Parameters common to all regions: κ_{PTCCI}, $\kappa_{\mathrm{CI}ptc}$, $\kappa_{\mathrm{CN}ptc}$, $\kappa_{\mathrm{WG}en}$, and $\kappa_{\mathrm{CN}en}$

Parameters	Intervals
κ_{PTCCI}	$(0, \min\{F_{\mathrm{PTC}_{1,\mathrm{T}}}, F_{\mathrm{PTC}_{2,\mathrm{T}}}\}]$
$\kappa_{\mathrm{CI}ptc}$	$\left(0, \min\left\{\frac{U_i}{1+Q_i H_{\mathrm{CI}} C_{\mathrm{CI}}}\right\}\right]$
$\kappa_{\mathrm{CN}ptc}$	$\left(\max\left\{\frac{U_i Q_i H_{\mathrm{CI}} C_{\mathrm{CI}}}{1+Q_i H_{\mathrm{CI}} C_{\mathrm{CI}}}\right\}, 1\right]$
$\kappa_{\mathrm{WG}en}$	$(0, w_2\beta_{\mathrm{med}}]$
$\kappa_{\mathrm{CN}en}$	$\left(0, \min_{i=1,2}\left\{\frac{U_i Q_i H_{\mathrm{CI}} C_{\mathrm{CI}}}{1+Q_i H_{\mathrm{CI}} C_{\mathrm{CI}}}\right\}\right]$ if $\kappa_{\mathrm{WG}en} \in [w_2\beta_{\min}, w_2\beta_{\mathrm{med}}]$
	$\left(0, \min_{i=1,2,4}\left\{\frac{U_i Q_i H_{\mathrm{CI}} C_{\mathrm{CI}}}{1+Q_i H_{\mathrm{CI}} C_{\mathrm{CI}}}\right\}\right]$ if $\kappa_{\mathrm{WG}en} \in (0, w_2\beta_{\min}]$

Let $w_2 \in \left\{\frac{\alpha_{\mathrm{CI}}}{1+\alpha_{\mathrm{CI}}}, \frac{\alpha_{\mathrm{WG}}}{1+\alpha_{\mathrm{WG}}}, \frac{\alpha_{\mathrm{WG}}+\alpha_{\mathrm{CI}}}{1+\alpha_{\mathrm{WG}}+\alpha_{\mathrm{CI}}}\right\}$

Table 4 Parameter $\kappa_{\mathrm{WG}wg}$ in each region

Region	Intervals
$G_k, k = \mathrm{I}, \ldots, \mathrm{VIII}b$	$[w_{2;C}\gamma_{\max}, 1]$ (cubitus pathway only)
	$[w_{2,C,W}\gamma_{\mathrm{med}}, w_{2;C,W}\gamma_{\max}]$ (both cubitus and wingless pathways)
G_{Auto}	$[w_{2;W}\gamma_{\mathrm{med}}, w_{2;W}\gamma_{\max}]$

In regions G_1 to $G_{\mathrm{VIII}b}$ the cubitus pathway contributes to wingless mRNA regulation. In region G_{Auto} only the wingless pathway contributes to wingless mRNA regulation. Define: $w_{2;C} = \frac{\alpha_{\mathrm{CI}}}{1+\alpha_{\mathrm{CI}}}$, $w_{2;C,W} = \frac{\alpha_{\mathrm{WG}}+\alpha_{\mathrm{CI}}}{1+\alpha_{\mathrm{WG}}+\alpha_{\mathrm{CI}}}$, and $w_{2;W} = \frac{\alpha_{\mathrm{WG}}}{1+\alpha_{\mathrm{WG}}}$

Table 5 Parameters κ_{CNwg} and κ_{CIwg} in each region

Region	Intervals	
	κ_{CNwg}	κ_{CIwg}
G_{I} ($\max_{i=1,4} \tilde{U}_i < \tilde{U}_2$)	$[\tilde{U}_2, 1]$	$[\max_{i=1,4}(U_i - \tilde{U}_i), U_2 - \tilde{U}_2]$
G_{II} ($\tilde{U}_4 < \tilde{U}_2 < \tilde{U}_1$)	$[\tilde{U}_2, \tilde{U}_1]$	$[U_4 - \tilde{U}_4, U_2 - \tilde{U}_2]$
G_{III} ($\tilde{U}_2 < \min_{i=1,4} \tilde{U}_i$)	$[\tilde{U}_2, \min_{i=1,4} \tilde{U}_i]$	$(0, U_2 - \tilde{U}_2]$
G_{IV} ($\tilde{U}_1 < \tilde{U}_2 < \tilde{U}_4$)	$[\tilde{U}_2, \tilde{U}_4]$	$[U_1 - \tilde{U}_1, U_2 - \tilde{U}_2]$
$G_{\mathrm{V}a}$ ($\tilde{U}_4 = \tilde{U}_2 < \tilde{U}_1$)	$\{\tilde{U}_2\}$	$(0, U_2 - \tilde{U}_2]$
$G_{\mathrm{V}b}$ ($\tilde{U}_4 = \tilde{U}_2 < \tilde{U}_1$)	$[\tilde{U}_2, \tilde{U}_1]$	$\{U_2 - \tilde{U}_2\}$
$G_{\mathrm{VI}a}$ ($\tilde{U}_4 < \tilde{U}_2 = \tilde{U}_1$)	$\{\tilde{U}_2\}$	$[U_4 - \tilde{U}_4, U_2 - \tilde{U}_2]$
$G_{\mathrm{VI}b}$ ($\tilde{U}_4 < \tilde{U}_2 = \tilde{U}_1$)	$[\tilde{U}_2, 1]$	$\{U_2 - \tilde{U}_2\}$
$G_{\mathrm{VII}a}$ ($\tilde{U}_1 = \tilde{U}_2 < \tilde{U}_4$)	$\{\tilde{U}_2\}$	$(0, U_2 - \tilde{U}_2]$
$G_{\mathrm{VII}b}$ ($\tilde{U}_1 = \tilde{U}_2 < \tilde{U}_4$)	$[\tilde{U}_2, \tilde{U}_4]$	$\{U_2 - \tilde{U}_2\}$
$G_{\mathrm{VIII}a}$ ($\tilde{U}_1 < \tilde{U}_2 = \tilde{U}_4$)	$\{\tilde{U}_2\}$	$[U_1 - \tilde{U}_1, U_2 - \tilde{U}_2]$
$G_{\mathrm{VIII}b}$ ($\tilde{U}_1 < \tilde{U}_2 = \tilde{U}_4$)	$[\tilde{U}_2, 1]$	$\{U_2 - \tilde{U}_2\}$
G_{Auto}	$(0, \tilde{U}_i]$ or	$[U_i - \tilde{U}_i, 1]$ (each $i = 1, 2, 4$)

In regions G_I to G_{VIII} the cubitus pathway contributes to wingless mRNA regulation. In region G_{Auto} only the wingless pathway contributes to wingless mRNA regulation. Define $\tilde{U}_i = \frac{U_i Q_i H_{\mathrm{CI}} C_{\mathrm{CI}}}{1 + Q_i H_{\mathrm{CI}} C_{\mathrm{CI}}}$, and note that $U_i - \tilde{U}_i = \frac{U_i}{1 + Q_i H_{\mathrm{CI}} C_{\mathrm{CI}}}$

are reduced to:

$$\kappa_{\mathrm{WG}en} \leq wg_2 \beta_{\mathrm{med}},$$

$$\kappa_{\mathrm{CN}en} < \min\{\mathrm{CN}_1, \mathrm{CN}_2\},$$

$$\kappa_{\mathrm{WG}en} > wg_2 \beta_{\mathrm{min}} \quad \text{or} \quad \kappa_{\mathrm{CN}en} < \mathrm{CN}_4,$$

$$\kappa_{\mathrm{WG}wg} \leq wg_2 \gamma_{\mathrm{max}} \quad \text{or} \quad \min\{\kappa_{\mathrm{CN}wg}, U_2 - \kappa_{\mathrm{CI}wg}\} \geq \mathrm{CN}_2,$$

$$\kappa_{\mathrm{WG}wg} > wg_2 \gamma_{\mathrm{med}},$$

$$\min\{\kappa_{\mathrm{CN}wg}, U_1 - \kappa_{\mathrm{CI}wg}\} < \mathrm{CN}_1,$$

$$\min\{\kappa_{\mathrm{CN}wg}, U_4 - \kappa_{\mathrm{CI}wg}\} < \mathrm{CN}_4,$$

There are now three possibilities according to the value of wg_2, yielding the intervals listed in Tables 3, 4, and 5.

References

1. Alon U, Surette MG, Barkai N, Leibler S (1999) Robustness in bacterial chemotaxis. Nature 397:168–171
2. Little JW, Shepley DP (1999) Robustness of a gene regulatory circuit. EMBO J 18:4299–4307

3. von Dassow G, Meir E, Munro EM, Odell GM (2000) The segment polarity network is a robust developmental module. Nature 406:188–192

4. Kim J, Bates DG, Postlethwaite I, Ma L, Iglesias P (2006) Robustness analysis of biochemical network models. IEE Proc Syst Biol 153:96–104

5. Savageau MA (1971) Parameter sensitivity as a criterion for evaluating and comparing the performance of biochemical systems. Nature 229:542–544

6. Heinrich R, Schuster S (1996) The regulation of cellular systems. Chapman & Hall, New York

7. Sanson B (2001) Generating patterns from fields of cells. Examples from Drosophila segmentation. EMBO Rep 21:1083–1088

8. Ingolia NT (2004) Topology and robustness in the Drosophila segment polarity network. PLoS Biol 2:0805–0815

9. Albert R, Othmer HG (2003) The topology of the regulatory interactions predicts the expression pattern of the Drosophila segment polarity genes. J Theor Biol 223:1–18

10. Umulis D, O'Connor MB, Othmer H (2007) Robustness of embryonic spatial patterning in Drosophila melanogaster. Curr Top Dev Biol 81:65–111

11. Chaves M, Albert R, Sontag ED (2005) Robustness and fragility of boolean models for genetic regulatory networks. J Theor Biol 235:431–449

12. Chaves M, Sontag ED, Albert R (2006) Methods of robustness analysis for boolean models of gene control networks. IEE Proc Syst Biol 153:154–167

13. Ma W, Lai L, Ouyang Q, Tang C (2006) Robustness and modular design of the drosophila segment polarity network. Mol Syst Biol 2:70

14. Gutenkunst RN, Waterfall JJ, Casey FP, Brown KS, Myers CR, Sethna JP (2007) Universally sloppy parameter sensitivities in systems biology models. PLoS Comput Biol 3(10):e189+

15. Dayarian A, Chaves M, Sengupta A, Sontag ED (2008) Shape, size and robustness: feasible regions in the parameter space of biochemical networks. PLoS Comput Biol (in press)

16. Sengupta AM, Djordjevic M, Shraiman BI (2002) Specificity and robustness in transcription control network. Proc Natl Acad Sci USA 99:2072–2077

17. Hooper JE, Scott MP (1992) The molecular genetic basis of positional information in insect segments. In: Hennig W (ed) Early embryonic development of animals. Springer, Berlin, pp 1–49

18. Hidalgo A, Ingham PW (1990) Cell patterning in the Drosophila segment: spatial regulation of the segment polarity gene patched. Development 110:291–301

19. Eaton S, Kornberg TB (1990) Repression of ci-d in posterior compartments of drosophila by engrailed. Genes Dev 4:1068–1077

20. von Dassow G, Odell GM (2002) Design and constraints of the drosophila segment polarity modude: robust spatial patterning emerges from intertwined cell state switches. J Exp Zool (Mol Dev Evol) 294:179–215

21. Swantek D, Gergen JP (2004) Ftz modulates runt-dependent activation and repression of segment -polarity gene transcription. Development 131:2281–2290

22. Collins GE (1975) Quantifier elimination for real closed fields by cylindrical algebraic decomposition. In: Second GI Conference on Automata Theory and Formal Languages, Kaiserslauten. Lecture Notes Comp. Sci., vol 33 Springer, Heidelberg, pp 134–183

23. Arnon DS, Collins GE, McCallum S (1984) Cylindrical algebraic decomposition I: the basic algorithm. SIAM J Comput 13:865–877

24. Brown C, Hong, et al. H QEPAD. http://www.cs.usna.edu/qepcad/B/QEPCAD.html

25. Collins GE, Hong H (1991) Partial cylindrical algebraic decomposition in quantifier elimination. J Symb Comput 12:299–328

26. Wolfram S (1998) The Mathematica Book, 4th edn. Wolfram Media, Cambridge University Press, London

27. Nešić D, Mareels IMY, Glad ST, Jirstrand M (2001) Software for control system analysis and design, symbol manipulation. In: Webster J (ed) Encyclopedia of electrical and electronics engineering. Wiley, London

28. Lafferriere G, Pappas G, Yovine S (2001) Symbolic reachability computation for families of linear vector fields. J Symb Comput 32:231–253

29. Ghosh R, Tomlin CJ (2004) Symbolic reachable set computation of piecewise affine hybrid automata and its application to biological modeling: Delta-notch protein signaling. IEE Trans Syst Biol 1: 170–183